DOI: 10.1534/genetics.105.047100

Mutational Analysis of *Stubble-stubbloid* Gene Structure and Function in Drosophila Leg and Bristle Morphogenesis

Ann S. Hammonds and James W. Fristrom[1]

Department of Molecular and Cell Biology, University of California, Berkeley, California 94720

Manuscript received June 23, 2005
Accepted for publication November 11, 2005

ABSTRACT

The *Stubble-stubbloid* (*Sb-sbd*) gene is required for ecdysone-regulated epithelial morphogenesis of imaginal tissues during Drosophila metamorphosis. Mutations in *Sb-sbd* are associated with defects in apical cell shape changes critical for the evagination of the leg imaginal disc and with defects in assembly and extension of parallel actin bundles in growing mechanosensory bristles. The *Sb-sbd* gene encodes a type II transmembrane serine protease (TTSP). Here we use a *Sb-sbd* transgenic construct to rescue both bristle and leg morphogenesis defects in *Sb-sbd* mutations. Molecular characterization of *Sb-sbd* mutations and rescue experiments with wild-type and modified *Sb-sbd* transgenic constructs show that the protease domain is required for both leg and bristle functions. Truncated proteins that express the noncatalytic domains without the protease have dominant effects in bristles but not in legs. Leg morphogenesis, but not bristle growth, is sensitive to *Sb-sbd* overexpression. Antibody localization of the Sb-sbd protein shows apical expression in elongating legs. Sb-sbd protein is found in the base and shaft in budding bristles and then concentrates at the growing tip when bristles are elongating rapidly. We propose a model whereby *Sb-sbd* helps coordinate proteolytic modification of extracellular matrix attachments with cytoskeletal changes in both legs and bristles.

ELABORATE changes in the dimensions and topology of epithelial sheets are required for the normal development of multicellular organisms; developmental events as basic as gastrulation and as specialized as the formation of the stereocilia of the mammalian inner ear are examples of epithelial morphogenesis. Cell division and death, cell rearrangement, and cell-shape change all contribute to different types of epithelial morphogenesis (reviewed in Fristrom 1988). These cell behaviors depend in part on changes in the cytoskeleton but occur in the context of neighboring cells, extracellular matrices (ECM), and hormonal milieus. Drosophila imaginal discs provide an attractive experimental system to study the complex interrelationships of the cytoskeleton, ECM, cell junctions, and extracellular signals during epithelial morphogenesis in a genetically tractable model organism.

During metamorphosis in Drosophila, the adult epidermis is pieced together from a collection of anlagen, the imaginal (adult) discs. Imaginal discs are simple, folded epithelial sacs which, in response to the metamorphic steroid hormone 20-hydroxyedcysone (ecdysone), undergo rapid and radical tissue reorganization to form specific structures of the adult integument. The thoracic imaginal discs give rise to the adult thoracic appendages (legs, wings, and halteres); their proximal parts fuse to form the epidermis of the thorax. The initial transformation from folded, undifferentiated imaginal discs to appendages with the basic shape of the adult structures takes place in the prepupal period, the first 12 hr after pupariation (AP). Following the ecdysone-triggered transition to the 84-hr pupal period, the appendage morphology is further refined, bristles and hairs form, and finally the adult cuticle is deposited.

Significant progress has been made in understanding how the ecdysone receptor and its partner ultraspirical interact with nuclear receptor cofactors and ecdysone-induced transcription factors to confer temporal and tissue specificity onto signals from this single hormone (reviewed in Thummel 1997, 2002). Less is known about products of the effector genes, molecules that have a direct function in cell and tissue morphogenesis. Genetic interaction screens, pioneered in our laboratory, have identified some of the genes that act in imaginal disc morphogenesis (Beaton *et al.* 1988; Gotwals and Fristrom 1991; Clark *et al.* 1995; Edwards and Kiehart 1996; Gates and Thummel 2000; Bayer *et al.* 2003; Ward *et al.* 2003; Chen *et al.* 2004). A role for the *Stubble-stubbloid* (*Sb-sbd*) gene in leg and wing morphogenesis was discovered in the first of these studies (Beaton *et al.* 1988).

Sb-sbd transcription is induced by ecdysone and is required both in prepupae, for the initial elongation of the leg disc to form a tubular leg, and in pupae (32 hr

[1]*Corresponding author:* Department of Molecular and Cell Biology, 569 Life Science Addition, University of California, Berkeley, CA 94720-3200. E-mail: jfristro@calmail.berkeley.edu

AP), for the apical extension of a single cell to form the mechanosensory bristle shaft (Appel *et al.* 1993). Bristle phenotypes are distinct in dominant (*Sb*) and recessive (*sbd*) mutations. Defects in leg morphogenesis are recessive in all *Sb-sbd* mutants (Table 1).

In prepupae the leg disc telescopes out of the concentrically folded epithelium to form a cylinder and everts to the outside of the developing imago. This change in tissue shape results primarily from changes in cell shape (Condic *et al.* 1991; Fristrom and Fristrom 1993). At the end of the third instar, cells that will form the basitarsis and distal tibia maintain an anisometric shape with the proximal-distal axis compressed and the circumferential axis elongated. By 6 hr AP, the leg has become tubular and the elongated cells have become isometric, the change in cell shape, longer in the proximal-distal direction and narrower in width, mediating the change in tissue shape. In *Sb-sbd* mutants, these cell-shape changes are limited and the legs of the adult exhibit the malformed (mlf) phenotype with leg segments that are short, thick, and often kinked or gnarled (see Beaton *et al.* 1988, Figure 1).

In pupae, each bristle develops as an apical cytoplasmic extension of a tricogen cell, one of the four cells that make up the mechanosensory bristle organ (Lees and Waddington 1942; Lees and Picken 1945; Hartenstein and Posakony 1989; Tilney *et al.* 1995). Within the extending bristle cell, a scaffold is formed by a core of microtubules surrounded by modules of membrane-associated actin microfilament bundles joined end to end (Overton 1967; Appel *et al.* 1993; Tilney *et al.* 1995, 1996, 1998; Wulfkuhle *et al.* 1998). The bristle grows as individual actin filaments continuously form at the bristle tip on the cytoplasmic side of the plasma membrane and are gathered together to form progressively larger and more tightly crosslinked bundles by the sequential action of two actin-binding proteins, forked and singed (Lees and Picken 1945; Tilney *et al.* 1996). Once the bristle is fully elongated, a chitinous cuticle is secreted and the actin bundle scaffolding is dismantled (Tilney *et al.* 1996, 2003; Guild *et al.* 2002). Bristles of *Sb* mutants are short, thick, and blunt ended. In these developing bristles the number of actin bundles is increased and in the most severe alleles, the bundles are also disorganized, with some bundles in the center of the bristle rather than regularly distributed around the cell perimeter (Lees and Picken 1945; Appel *et al.* 1993). Developing bristles in recessive *sbd* mutants start out with the normal number and distribution of actin bundles, but the bundles become deranged at the tip and stop prematurely and asynchronously (Appel *et al.* 1993). Reflecting this developmental defect, bristles of the homozygous *sbd* adults are short but with slightly tapered and frayed ends (see Appel *et al.* 1993, Figure 5).

The *Sb-sbd* protein (which for convenience we will refer to as stubblin) is the first identified invertebrate member of the type II transmembrane serine proteases (TTSP), each containing a C-terminal extracellular serine protease domain, a short N-terminal intracellular domain, and a variety of structural motifs connecting the transmembrane domain with the catalytic domain (Hooper *et al.* 2001; Netzel-Arnett *et al.* 2003). The modular structure of these proteases suggests a possible role linking proteolysis of the ECM to cytoskeletal rearrangements. Like other members of the TTSP family, the predicted 786-aa stubblin (Figure 2) includes an N-terminal cytoplasmic domain, followed by a transmembrane signal/anchor domain and an extracellular stem region with a C-terminal serine protease domain (Appel *et al.* 1993; Hooper *et al.* 2001). The 244-aa protease domain shares extensive sequence similarity to the S1 family (clan SA) of trypsin-like proteases (Furie and Furie 1988; Rawlings *et al.* 2004) in the conserved regions of the substrate-binding pocket, cleavage activation site, and catalytic triad, indicating a preference for cleavage after arginine or lysine. Commonly, these proteases are zymogens that are activated by cleavage at a characteristic activation site motif. In some proteases with a long prodomain, the noncatalytic domain remains tethered via a disulfide bond to the catalytic domain after cleavage (Rawlings *et al.* 2004). In stubblin, Cys-531 and Cys-659 are appropriately placed to provide this function. In the extracellular region just beyond the transmembrane domain, a conserved pattern of three pairs of cysteines defines a disuflide knot domain (or CLIP domain) like that found in several other arthropod proteases, including Limulus proclotting enzyme and the Drosophila snake and easter proteins, both secreted proteases involved in embryonic dorsal/ventral patterning (Gay and Keith 1992; Smith and DeLotto 1992; Muta *et al.* 1993; Jiang and Kanost 2000). The disulfide knot has been proposed to act as a binding site for a protease activator (Muta *et al.* 1990). For successful transgenic rescue of *snake* mutants, the *snake* transgenic construct must include an intact knot domain (Smith *et al.* 1994). A long serine/threonine-rich stem (aa 260–480) connects the stubblin knot and the protease. A similar, although shorter, region is essential for snake function (Smith *et al.* 1994).

Initial molecular studies of the *Sb-sbd* gene showed that the most severe dominant mutants were characterized by DNA insertions between the stem and the protease domain (Appel *et al.* 1993). The dominant bristle phenotype in these mutants suggests that one or more of the noncatalytic domains have a function either independent of (neomorphic) or antagonistic to (antimorphic) the wild-type bristle function. The observation that this apparent defect in the extracellular portion of the protein has a specific effect (formation of additional bundles) on the assembly of actin filaments inside the cell raised the possibility that *Sb-sbd* may be involved in an outside-to-inside signal, perhaps coordinating bristle elongation with proteolytic modification of the

surrounding apical ECM. The malformed leg phenotype, but not the bristle phenotype, in *Sb-sbd* mutants is enhanced in the presence of mutations in genes involved in myosin II-driven apical cell-shape change, including *zipper* (*zip*), the gene coding for nonmuscle myosin II heavy chain (Gotwals and Fristrom 1991; Bayer *et al.* 2003), reflecting the difference between apical cytoskeletal contraction in the elongating leg disc and formation of a long apical cytoplasmic extension by assembly and extension of parallel actin bundles in the developing bristle.

We took advantage of the differences in the bristle and leg roles for *Sb-sbd* to begin to connect biological functions to specific domains of stubblin. We have identified the molecular defects in three dominant *Sb* mutants and found that the most severe entirely lack a protease domain, while a mild allele is a frameshift mutation that adds a C-terminal hydrophobic sequence to the protease domain, arguably disabling the protease by interfering with folding and transmembrane processing. A severe recessive *sbd* mutant has a single base change likely to reduce but not eliminate protease function. Using transgenic lines expressing wild-type *Sb-sbd*, protease-disabled *Sb-sbd*, and a series of truncations, we show that a functional stubblin protease domain is required for both leg and bristle morphogenesis. Expression of truncated transgenes in a wild-type background generates *Sb*-like bristles, but not malformed legs. Antibody localization of stubblin in developing bristles of wild-type and *Sb* mutants indicates that the stubblin knot and/or stem domains help localize protease activity to the growing bristle tip. Surprisingly, overexpression of wild-type *Sb-sbd* has dominant effects on leg but not bristle morphogenesis during specific sensitive periods in both prepupal and pupal development. These results, taken in light of recently reported genetic interaction studies of *Sb-sbd* and Rho-signaling pathway mutations (Halsell *et al.* 2000; Bayer *et al.* 2003; Ward *et al.* 2003; Chen *et al.* 2004), suggest that *Sb-sbd* may coordinate ECM remodeling and cytoskeletal reorganization in both legs and bristles.

MATERIALS AND METHODS

Drosophila stocks: Drosophila *Sb-sbd* stocks used in this study are described in Beaton *et al.* (1988) and Table 1. Wild-type strains used were Oregon-R and Canton-S lines that have been maintained in our laboratory since 1964 and 1979, respectively. Transgenic stocks are described below. Stocks were maintained on standard cornmeal–agar medium at either 25° or 18°.

Transgenic constructs: See Figure 3. Generation of the wild-type *Sb-sbd* transgene (*hs-Sb-sbd*$^{+}$) was described previously (Hammonds 2002; Bayer *et al.* 2003). Briefly, full-length *Sb-sbd* cDNA (Appel *et al.* 1993) was cloned into a pLitmus 29 Vector (New England Biolabs, Beverly, MA) and then into the heat-shock-inducible *P*-element transformation vector pCaSpeR-hs (Thummel and Pirrotta 1992) to enable expression of the transgene under heat-shock control. The pLitmus29 *Sb-sbd* cDNA clone was used as a mutagenesis template to construct modified *Sb-sbd* transgenes, which were subsequently cloned into pCaSpeR-hs and injected into w^{1118} embryos using standard methods (Rubin and Spradling 1982). The protease-disabled S737A construct, which substitutes an alanine for the catalytic serine at amino acid 737, was made from the wild-type template using QuikChange mutagenesis (Stratagene, La Jolla, CA) to change Ser (TCA) to Ala (GCA) using the primer 5′-TGTCAGGGCGATGCAGGAGGTCC-3′. The truncated Sb transgene *hs-Sb-Δprotease* deletes the wild-type *Sb-sbd* cDNA coding for the protein sequence C-terminal to amino acid 517 and so lacks the entire protease domain. The truncated Sb-transgene *hs-SbCD-TM-knot* deletes the DNA coding for the protein sequence C-terminal of residue 257, so that only the cytoplasmic domain, the transmembrane domain, and the disulfide knot remain. The *hs-SbCD* and *hs-SbCD-TM* stocks were gifts from C. Bayer. The *hs-SbCD* construct includes only the cytoplasmic domain while *hs-SbCD-TM* retains the cytoplasmic domain with the transmembrane domain and some extracellular sequence but excludes the disulfide knot. Expression of transgenic protein products was confirmed by Western blotting for the *hs-Sb-sbd*$^{+}$, *hs-Sb-Δprotease*, and *hs-Sb-S737A* constructs. The shorter truncations do not contain the epitope against which our antibody was generated so their expression cannot be verified and results with these constructs must be considered preliminary.

Heat-shock protocol: Animals were staged from white prepupae (WPP) and heat-shocked immediately for the 0-hr time point or kept at 25° until the desired age, described in hours AP. The collected WPP were placed onto the walls of standard plastic food vials. For heat shocks the vials were immersed in a 37° water bath for 60 min. After heat shock the vials were returned to 25° until the adults eclosed. Adults were then scored for bristle or leg phenotype.

Sequence analysis of *Sb-sbd* mutants: To identify sequence defects in *Sb-sbd* mutants, genomic DNA from each homozygote mutant (Sb^{spike}, sbd^{2}, sbd^{201}, and the sbd^{201} progenitor br^{1}) was amplified using *Sb-sbd* exon-specific primers. All sequences were determined in both directions. Mutations and polymorphisms were verified by sequencing independent PCR products using at least two different primer pairs. The 3′-ends of Sb^{63b} and Sb^{70} cDNA were isolated from homozygote WPP total RNA by 3′-RACE PCR (Frohman 1993) using reagents from the Invitrogen (Carlsbad, CA) 3′-RACE kit. First-strand cDNA synthesis was primed with an oligo(dT) primer containing an adaptor sequence at its 5′-end. The PCR step used a 5′ primer from exon 5 in the *Sb-sbd* stem region (nt 1558–1773) and the adaptor sequence as the reverse primer. This PCR product was then cloned into a PCRII vector (Invitrogen) and sequenced. Manual double-stranded sequencing was done with the dideoxy chain termination method using Sequenase version 2 kit (USB, Cleveland). Automated sequencing was done at the University of California DNA sequencing facility. PCR and sequencing primers were made by GIBCO–BRL/Invitrogen or the University of California Cancer Research Laboratory Microchemical Facility. DNA sequence analysis was facilitated by the use of MacVector sequence analysis software (Oxford Molecular Group/Accelrys, San Diego) and the NCBI BLAST server.

Preparation of antibodies: A 26-amino-acid synthetic peptide from a nonrepetitive region in the stubblin stem was used to generate polyclonal antisera in guinea pigs (see Figure 3). The stem peptide was a generous gift of D. King. Antisera were prepared by Covance Research Services (Richmond, CA).

Dissection and antibody staining of imaginal discs: White prepupae were collected and either dissected immediately or aged for 1–4 hr at 25°. The disc–brain complex was dissected in Drosophila Ringers (130 mm NaCl, 5 mm KCl, 1.5 mm $CaCl_2$) and fixed for 30 min in 4% formaldehyde in TBS pH 7.6

TABLE 1

Leg and bristle phenotypes of *Sb-sbd* mutant alleles

Allele/genotype	Phenotype		Origin	Reference
	Bristle	Leg		
Sb^{63b}			Transposon	Appel *et al.* (1993)
Sb^{63b}/+	<1/2 wt length, thicker than wt, ends blunt	wt		Beaton *et al.* (1988)
Sb^{63b}/*Sb^{63b}*	<1/4 wt length, thicker than wt, ends blunt	mlf		Beaton *et al.* (1988)
Sb^{63b}/*Df (3R)sbd^{105}*	<1/4 wt length, thicker than wt, ends blunt	mlf		Beaton *et al.* (1988)
Sb^{1}			Transposon	Appel *et al.* (1993)
Sb^{1}/+	~1/2 wt length, thicker than wt, ends blunt	wt		Beaton *et al.* (1988)
Sb^{1}/*Sb^{1}*	(Lethal)			Dobzhansky (1929)
Sb^{1}/*Df (3R)sbd^{105}*	(Lethal)			Beaton *et al.* (1988)
Sb^{1}/*Sb^{63b}*	<1/4 wt length, thicker than wt, ends blunt	mlf		Beaton *et al.* (1988)
Sb^{spike}			X ray	Moore (1935)
Sb^{spi}/+	<2/3 wt length, ends blunt	wt		Beaton *et al.* (1988)
Sb^{spi}/*Sb^{spi}*	~1/4 wt length, ends blunt	mlf		R. Abu-Shumays and D. Fristrom (unpublished results)
Sb^{spi}/*Df(3R)sbd^{105}*	~1/4 wt length, ends blunt	mlf		Beaton *et al.* (1988)
Sb^{70}			Transposon	Appel *et al.* (1993)
Sb^{70}/+	<1/2 wt length, thicker than wt, ends blunt	wt		Beaton *et al.* (1988)
Sb^{70}/*Sb^{70}*	<1/4 wt length, thicker than wt, ends blunt	mlf		Beaton *et al.* (1988)
Sb^{70}/*Df(3R)sbd^{105}*	<1/4 wt length, thicker than wt, ends blunt	mlf		Beaton *et al.* (1988)
sbd^{2}			Spontaneous	Lindsley and Grell (1968)
sbd^{2}/+	wt	wt		Beaton *et al.* (1988)
sbd^{2}/*sbd^{2}*	~3/4 wt length, ends uneven	wt		Beaton *et al.* (1988)
sbd^{2}/*Df(3R)sbd^{105}*	~3/4 wt length, ends uneven	wt		Beaton *et al.* (1988)
sbd^{201}			EMS	Beaton *et al.* (1988)
sbd^{201}/+	wt	wt		Beaton *et al.* (1988)
sbd^{201}/*sbd^{201}*	<1/2 wt length, ends uneven	mlf		Beaton *et al.* (1988)
sbd^{201}/*Df(3R)sbd^{105}*	<1/2 wt length, ends uneven	mlf		Beaton *et al.* (1988)
Df(3R)sbd^{105}			X ray	Lewis (1948)
Df(3R)sbd^{105}/*wt*	wt	wt		Beaton *et al.* (1988)
Df(3R)sbd^{105}/*Df(3R)sbd^{105}*	(Lethal)			Beaton *et al.* (1988)

wt, wild type.

(20 mM Tris, 137 mM NaCl) at room temperature on a rocker. The fixed tissue was washed three times in TBS and then transferred to blocking solution (2% goat serum, 1% BSA in TBS). In the block, the discs were separated from the brain and any other adhering tissues. The cleaned discs were transferred to a fresh block and incubated, rocking, at room temperature for a total of 2 hr. Discs were then incubated overnight at 4° in stubblin antibody diluted 1:400 in blocking solution. Primary antibody was washed out with five washes of TBS. After a 15-min blocking step, discs were incubated for 1.5 hr in secondary antibody, fluorescein-conjugated anti-guinea pig IgG (H + L), affinity purified (Vector Laboratories, Burlingame, CA), and used at 20 μg/ml. Discs were then washed five times with TBS. After the last wash, TBS was replaced with 25% glycerol in TBS and the discs were allowed to equilibrate for 5 min. Discs were mounted on slides with Vectashield mounting medium (Vector Laboratories, Burlingame, CA).

Dissection and antibody staining of developing bristles: Pupae were staged from WPP and aged at 25° for 32–48 hr or at 18° to an equivalent developmental stage. Thoraces were dissected using a modification of the method described by Tilney *et al.* (1996). Pupae were placed on double-stick tape and pupal cases were removed. Dorsal thoraces were collected as described (Tilney *et al.* 1996) except that cleaning of the tissue was delayed until after a longer initial fixation step: 30 min at room temperature and then 2 hr to overnight at 4°. Following fixation, the large tracheoles and fat body were removed, and the pupal cuticle was gently peeled away from the epidermis. The fixed, cleaned thoraces were incubated in 0.1% Triton X-100, 4% formaldehyde in TBS for 20 min and then washed five times in TBS, 0.1% Triton. For antibody staining, thoraces were incubated in blocking solution (1% BSA, 2% goat serum in TBS) for 1.5 hr and then in antibody solution overnight at 4° at the same dilutions as used for disc staining. Secondary antibody incubations and subsequent washes were done as for disc staining. For mounting, a final 40% glycerol equilibration step was added before mounting in Vectashield mounting medium diluted 1:1 in TBS. For phalloidin staining of actin, fixed and permeablized thoraces were incubated 2 hr at room temperature or overnight at 4° in phalloidin conjugated to either Texas Red or fluorescein (Molecular Probes, Eugene, OR) and diluted into 4% formaldehyde in TBS and then washed and mounted as for antibody-stained tissues.

Conventional fluorescence and confocal microscopy: Slides were examined with both conventional fluorescence microscopy on a Zeiss Axiophot microscope and scanning laser confocal microscopy using a Bio-Rad (Hercules, CA) 1024 confocal microscope and COMOS software. Confocal images were processed and analyzed using either NIH Image 1.62 or Photoshop 3.0.5 (Adobe, San Jose, CA).

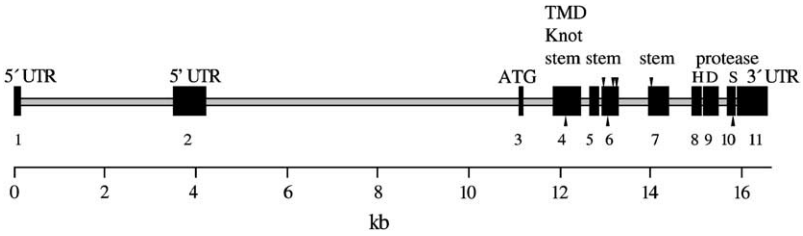

FIGURE 1.—*Sb-sbd* genomic structure. Sizes of exons and introns are represented to scale and indicated in kilobases at the bottom. Exons are shown as solid bars with exon number below. Features from the cDNA (5′- and 3′-UTR, ATG translation start) and amino acid sequence are indicated above the exons in which they are found. The protease domain is split among the last four exons. Each of the amino acids forming the catalytic triad (H, D, S) is encoded in a separate exon, indicated by marks above the appropriate exon. The transmembrane signal/anchor (TMD), disulfide knot (knot), and the first part of the stem are in exon 4. See text and Figure 2 for further description of protein domains. Four polymorphisms that result in a change in amino acid sequence are found in exons 6 and 7 and are indicated by marks above the line. In exon 6, an in-frame deletion of CAG in the Oregon-R strain reduces a string of seven glutamines to six between amino acids 287 and 293. An A-to-T change at nucleotide 1910 (cDNA numbering) results in a serine-for-threonine substitution at amino acid 349 within a serine/threonine (S/T)-rich region. At nucleotide 1924, a C-to-T change replaces a proline with a serine at amino acid 354. In exon 7, a third wild-type strain (the progenitor for the sbd^{201} mutant) deletes nine nucleotides inframe, resulting in the deletion of one unit of a tandem repeat of threonine, threonine, serine (TTS), between amino acids 410 and 416 in an S/T-rich region. Nucleotide differences between the Oregon-R and *y; cn bw sp* strains that produce no amino acid changes are found in exon 4 (nt 1150), exon 6 (nt1859), and exon 10 (nt 2198) and are indicated by marks below the exons.

RESULTS

***Sb-sbd* genomic structure and polymorphisms:** The sequence of the *Sb-sbd* cDNA and the preliminary genomic structure were published previously (APPEL *et al.* 1993). These results have been revised and extended (Figure 1). Several polymorphisms were found when the cDNA sequence (APPEL *et al.* 1993; gi 158511) from a wild-type Oregon-R strain was compared to the published genomic sequence from a *y; cn bw sp* strain (ADAMS *et al.* 2000; gi 7300108). Four changes, all in exons 6 or 7 of the repetitive stem region, result in amino acid sequence differences (Figure 1). The concentration of polymorphisms in the stem exons, including nonconservative substitutions (*e.g.*, a proline to serine at aa 349), suggests that the function of the stem tolerates sequence and secondary structure variation.

Molecular characterization of *Sb-sbd* mutations: To address specifically the basis of the differences between the effects of dominant and recessive mutants on leg morphogenesis and bristle development, we sequenced dominant (*Sb*) and recessive (*sbd*) alleles (Figure 2). The dominant alleles form an allelic series with respect to both bristle length and leg morphology. Sb^{63b} and Sb^{70} are equivalent and stronger than Sb^{1}, which in turn is more severe than Sb^{spike} (BEATON *et al.* 1988). Deficiencies for the locus (*e.g.*, sbd^{105}) have no dominant phenotype and have *sbd* bristles but are not malformed in heteroallelic combination with the mildest *sbd* allele, sbd^{2}. A more severe *sbd* allele, sbd^{201}, isolated on the basis of its malfomed leg phenotype in combination with br^{1}, is both *sbd* and malformed when heterozygous with a *Sb-sbd* deficiency (BEATON *et al.* 1988). Although it is a severe recessive allele, several genetic observations support the conclusion that sbd^{201} is not a null but an antimorph. First, compared to deficiencies for the *Sb-sbd* locus, sbd^{201} interacts with (*broad*) *br* and *zip* mutants

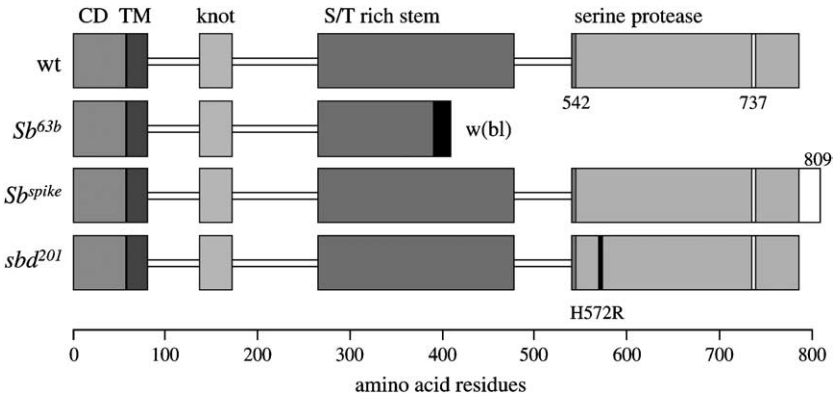

FIGURE 2.—Sequence changes in *Sb-sbd* mutants. Amino acid residue number is shown in the scale at the bottom. The top line shows protein domains of wild-type stubblin (wt): CD (cytoplasmic domain) aa 1–58, TM (transmembrane domain) aa 59–81, knot (disulfide-knotted domain) aa 138–173, S/T-rich (serine and threonine rich region of the stem) aa 260–480, and serine protease from activation cleavage site at aa 542 to the C terminus at aa 786. Position of the cleavage site is shown by a solid vertical bar and the catalytic serine at aa 737 is indicated by an open vertical bar. The truncated Sb^{63b} cDNA sequence contains sequence from the $white^{blood}$ transposable element after the end of exon 6 in the stem at *Sb-sbd* cDNA nucleotide 2028 (corresponding to aa 386). A stop occurs 22 codons into the $white^{blood}$ sequence. The amino acid residues from the $white^{blood}$ sequence are indicated by a solid bar. Sb^{70} cDNA is similarly truncated (see text). In Sb^{spike}, a frameshift mutation occurs in the C-terminal arginine codon (AGA to GAT), resulting in the substitution of an aspartic acid for the final arginine and the addition of 23 residues [(R786D)DDQKILTTADRLLLFVLIYQLYL]. The additional sequence extending the protein length to 809 residues is indicated by an open bar. sbd^{201} has a single base change (CAC to CGC) at nucleotide 2583, resulting in a substitution of arginine for histidine at aa 572, indicated by a solid vertical bar labeled H572R.

with greater penetrance to produce severely mlf legs (J. Fristrom, unpublished results). If it were a null, sbd^{201} would behave similarly to the deficiency. Similarly, a null sbd^{201} homozygote would be expected to have the same phenotype as sbd^{201} in heteroallelic combination with a *Sb-sbd* deficiency. Both of these combinations have a severe mlf leg phenotype like that of *Sb* dominant mutants either homozygous or in combination with a deficiency (Beaton *et al.* 1988). The bristle phenotype, however, is more severe in the sbd^{201} homozygote than in the deficiency *trans*-heterozygote (our unpublished observation), and unlike *Sb-sbd* deficiencies, sbd^{201} does not enhance the bristle phenotype of the mild hypomorph sbd^{2}. Thus, although the bristle phenotype in sbd^{201} mutants is recessive, sbd^{201} effects on bristles are different from those of a *sbd* deficiency and, with respect to the leg phenotype, sbd^{201} behaves more like the *Sb* alleles. For this reason, sbd^{201} was chosen for further sequence analysis along with sbd^{2} and the dominant mutants Sb^{63b}, Sb^{70}, and Sb^{spike}.

***sbd*^{201}:** Genomic DNA from sbd^{201} homozygotes and the progenitor stock for sbd^{201} was sequenced in both directions through the entire protein-coding region and the two 5′ untranslated exons. Two differences from the published wild-type *Sb-sbd* sequence were found. In exon 7, in an ST-rich region of the stem, sbd^{201} DNA contains an in-frame 9-bp deletion, which eliminates one STT repeat. This variation is also in the progenitor stock and so does not itself cause the *sbd* phenotype. The second and more significant difference is a single base change (A to G) at cDNA nucleotide 2583, resulting in an amino acid substitution of arginine (CGC) for histidine (CAC) at aa 572 (Figure 2). The progenitor stock for sbd^{201} has the wild-type sequence at this position. This amino acid is within a conserved region of the catalytic domain that forms the side of the P1′ pocket. This residue is equivalent to chymotrypsinogen His40, which has been proposed to have a role in stabilization of the zymogen by forming a hydrogen bond with Asp194 (Bode *et al.* 1978; Madison *et al.* 1993). Cleavage of the prodomain at the activation cleavage site disrupts this bond and leads to a conformational change that completes formation of the oxyanion hole and substrate-binding pockets. Alignment of all 29 mammalian TTSPs characterized to date (reviewed in Netzel-Arnett *et al.* 2003) shows that histidine 40 is conserved in 25 of these. Mouse and human matriptase substitute alanine and the enteropeptidases substitute leucine at this position. The histidine-to-arginine substitution in sbd^{201} may prevent the formation of a stable zymogen, resulting in nonspecific activation of the sbd^{201} protease, degradation of the protease, or both, or may disrupt prime-side substrate interactions to reduce effective substrate binding. Therefore, this mutation is likely to severely reduce but not completely eliminate stubblin protease activity.

***sbd*^{2}:** All 11 exons of the *Sb-sbd* cDNA, including the 9 protein-coding exons and both 5′ untranslated exons, were sequenced from sbd^{2}/sbd^{2} genomic DNA. The only detected coding sequence difference between sbd^{2} and the two published wild-type sequences (Oregon-R and *y; cn bw sp*) is the same STT deletion in exon 7 seen with sbd^{201} and its wild-type progenitor. Because it also occurs in wild-type flies, this deletion is not the cause of the mutant phenotype of sbd^{2}. No other alterations were found in the coding sequence. In the 697-bp intron between exons 6 and 7 in the stem, there is a tandem duplication of ggttctg not found in any sequenced wild-type strain; it is conceivable that this duplication may have a regulatory effect, such as disruption of an intronic enhancer binding site, although no specific regulatory function in this intron has been established. The possibility remains that there are changes in an as-yet-unidentified promoter region, splice junction, or other regulatory region. Considering that *Sb-sbd* deficiencies have a *sbd* phenotype, a regulatory mutation, particularly one that results in *Sb-sbd* underexpression, would be consistent with the mild hypomorphic phenotype of sbd^{2}/sbd^{2}.

***Sb* dominant mutations:** Three *Sb-sbd* mutations with dominant bristle phenotypes, Sb^{1}, Sb^{70}, and Sb^{63b}, are associated with insertions in the 3′ region of the *Sb-sbd* gene, in front of the catalytic domain (Appel 1992; Appel *et al.* 1993). Northern blots show that all three mutations produce truncated transcripts of ~2.8 kb instead of the wild-type 3.7-kb transcript (Abu-Shumays 1995). To identify the specific defect in the most severe mutation, Sb^{63b}, the 3′-end of the cDNA, isolated by RT–PCR from homozygote Sb^{63b}/Sb^{63b} white prepupal RNA, was sequenced. The shortened transcript matches *Sb* cDNA up to nucleotide 2028 (the end of exon 6, stem region) with 647 nucleotides from a $white^{blood}$ retroviral-like transposable element (Bingham and Chapman 1986) joined to the 3′-end. The combined $Sb{:}white^{blood}$ transcript is 2.7 kb, consistent with the ~2.8 kb-band seen on Northern blots (Appel *et al.* 1993; Abu-Shumays 1995). A stop codon occurs after 66 nucleotides of $white^{blood}$ sequence so that the protein product from this transcript could include up to 22 amino acids derived from the $white^{blood}$ insertion (Figure 2). The transition from *Sb-sbd* to $white^{blood}$ occurs at a splice junction, indicating that the transposable element is likely to be inserted in the intron preceding exon 7. Sequencing of Sb^{70}, which has a severe bristle phenotype like that of Sb^{63b}, identified a $white^{blood}$ insertion producing a similarly truncated $Sb{:}white^{blood}$ transcript. Unlike Sb^{63b}, however, Sb^{70} does not have a second insertion at the 5′-end of the gene (Appel 1992). The second insertion in Sb^{63b} has not been identified. It is successfully spliced out in white prepupal RNA detectable by Northern or RT–PCR (Abu-Shumays 1995). It should be noted that the $Sb{:}white^{blood}$ transcript is overexpressed approximately fourfold compared to the wild-type transcript in both $Sb^{63}/+$ and $Sb^{70}/+$ white prepupae (Abu-Shumays 1995).

Sb^{1} genomic DNA also contains an insertion before the beginning of the catalytic domain (Appel *et al.*

1993). Sb^{1}/+ flies have a milder bristle phenotype than Sb^{63b} or Sb^{70} heterozygotes and a weaker mlf leg phenotype in *trans*-heterozygote combinations. Sb^{1}/Sb^{1} homozygotes are lethal as early first instar larvae (data not shown). There is evidence that Sb^{1} lethality may be caused by closely linked but functionally independent loci (Appel 1992; Nelson and Szauter 1992; Hammonds 2002). Because the lethality of Sb^{1} homozygotes and the poor viability of the deficiency *trans*-heterozygotes make isolation of Sb^{1} RNA problematical, cDNA sequence analysis was not pursued for this mutant. However, the *trans*-heterozygote Sb^{1}/Sb^{63b} is weakly viable. Amplification of genomic DNA from these flies adjacent to and across the insertion site of the Sb^{63b} $white^{blood}$ element between exons 6 and 7 indicates that the Sb^{1} insertion also disrupts this region of the gene (data not shown), consistent with Southern analysis (Appel *et al.* 1993) and the 2.8-kb transcript size (Abu-Shumays 1995).

Sb^{spike} produces the wild-type-size 3.7-kb transcript (Abu-Shumays 1995). Both $Sb^{spike}/Df\ (3R)sbd^{105}$ *trans*-heterozygotes and Sb^{spike} homozygotes are viable and are mlf with a more severe bristle phenotype than $Sb^{spike}/+$. Exon-specific primers were used to amplify the *Sb-sbd* coding exons and the 3′ and 5′ untranslated regions from Sb^{spike}/Sb^{spike} genomic DNA . Three differences between the Sb^{spike}/Sb^{spike} DNA and the published wild-type sequences were detected. In exon 11, the Sb^{spike}/Sb^{spike} DNA sequence drops the A in the first position of the C-terminal arginine codon, resulting in a frameshift with the substitution of aspartic acid (GAT) for the arginine (AGA), substitution of another aspartic acid for the stop codon, and addition of 23 amino acids to the highly conserved protease domain before a new stop codon occurs (Figure 2). This appended sequence seems unlikely to be benign and may result in a complete loss of normal stubblin function. Of the first five residues, four are highly charged (DDDQK) and 11 of 12 of the last residues are hydrophobic (LLLFVLIYQLYL), suggesting that this sequence may interfere with processing of the protein through the membrane. In addition, the extra residues in the Sb^{spike} protease domain could disrupt effective folding, resulting in a change in the structure that alters or abolishes the protease function. Sb^{spike} DNA also contains an A-to-T substitution in the repetitive ST-rich region of exon 7 (stem), resulting in a threonine (ACA) being replaced by isoleucine (ATA) at aa 428. Because there are several differences in this region of the stem among the sequences of three wild-type strains, the additional residues at the end of the protease domain are more likely to be significant to the function of the protein. As well as these changes in the coding sequence, the intron between exons 6 and 7 contains the same 7-bp tandem repeat that is found in sbd^{2}. We have not ruled out the possibility that this duplication contributes to the hypomorphic phenotype of sbd^{2} and therefore also could be a factor in Sb^{spike}, for example, by reducing expression levels of the Sb^{spike} transcript and contributing to the observed milder (compared to Sb^{63b} and Sb^{70}) phenotype.

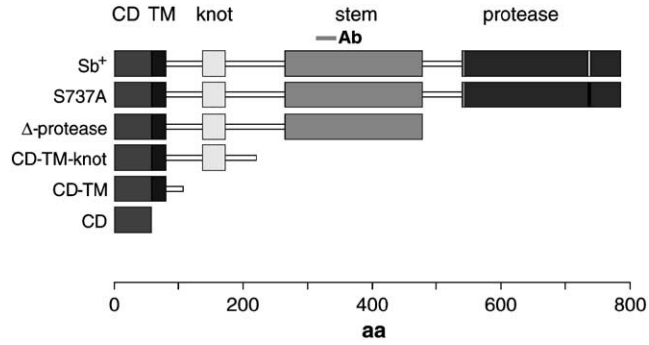

Figure 3.—*Sb-sbd* constructs for transgenic lines. Also shown is the location of the epitope for the stubblin stem (stem Ab) antiserum. The wild-type *Sb-sbd* (Sb^{+}) construct includes the full-length *Sb-sbd* cDNA. The protease-disabled construct (S737A) substitutes an alanine for the catalytic serine at aa 737. The Δ-protease construct deletes the wild-type cDNA coding for the protein sequence C-terminal of aa 517 and is therefore missing the entire protease domain. The CD–TM–knot construct deletes the wild-type cDNA coding for the protein sequence C-terminal to residue 257 and thus retains the cytoplasmic domain and extracellular sequence through the disulfide knot (knot), but deletes most of the S/T-rich stem and all of the protease domain. CD–TM also deletes the disulfide knot, and CD expresses only the intracellular domain. CD–TM and CD constructs were gifts from C. Bayer.

Rescue of Sb-sbd phenotypes with heat-shock-inducible *Sb-sbd* transgenes: Although the abundance of genomic mutational evidence supports the view that we have identified the structural *Sb-sbd* gene (Appel *et al.* 1993), the ultimate demonstration of gene identity is rescue of mutant phenotypes with the wild-type gene. Rescue of hypomorphic mutations and antimorphic mutations should be achievable with sufficient quantities of the wild-type gene product. Neomorphic mutations, with a qualitatively different function, should be resistant to rescue by the wild-type gene. To confirm by transgenic rescue that the phenotypes of the *Sb-sbd* recessive mutations result from insufficient wild-type *Sb-sbd* gene product, to replicate the bristle phenotypes of the *Sb* dominant mutations, and to initiate a structure/function analysis of the *Sb-sbd* gene, we constructed a series of *Sb-sbd* transgenes, shown in Figure 3. Wild-type *Sb-sbd* cDNA and a set of modified *Sb-sbd* cDNAs were cloned into a heat-shock-inducible transformation vector (see materials and methods) to allow expression of the transgenes during either leg morphogenesis (0–6 hr AP) or bristle formation (24–48 hr AP).

Rescue of bristle phenotypes: Table 2 shows rescue with a wild-type transgene of the bristle phenotype of the mild hypomorph sbd^{2} and the more severe mutant sbd^{2o1} with a single 1-hr heat shock at 27.5 hr AP, shortly before bristle nubs appear. With two copies of the transgene, 100% of the treated sbd^{2} flies had wild-type bristles. A single copy of the $hs\text{-}Sb\text{-}sbd^{+}$ transgene typically

TABLE 2

Rescue of bristle phenotype with heat-shock induction of wild-type *Sb-sbd* transgene

Genotype	Treatment	Bristle phenotype				
		n	% sbd	% Sb	% int	% wt
hs-Sb$^+$/*hs-Sb*$^+$;*sbd*^{2}/*sbd*^{2}	hs1	87	0	0	0	100
	No hs	53	100	0	0	0
hs-Sb$^+$/*hs-Sb*$^+$;*sbd*^{201}/*Df(3R)sbd*^{105}	hs1	50	0	0	10	90
	No hs	64	100	0	0	0
S737A/S737A; *sbd*^{2}/*sbd*^{2}	hs1	65	100	0	0	0
	No hs	86	100	0	0	0
hs-Sb$^+$/*hs-Sb*$^+$; *Sb*^{spike}/+	hs1	63	0	38	43	19
	No hs	72	0	100	0	0
hs-Sb$^+$/*hs-Sb*$^+$; *Sb*^{63b}/+	hs1	55	0	96	4	0
	hs2	58	0	100	0	0
	No hs	84	0	100	0	0

Homozygote *sbd*^{2}/*sbd*^{2}, deficiency *trans*-heterozygote *sbd*^{201}/*Df(3R)sbd*^{105} or heterozygote *Sb*^{63b}/+, and *Sb*^{spike}/+ stocks carrying two copies of the wild-type *Sb-sbd* transgene (hs-Sb$^+$/hs-Sb$^+$), and *sbd*^{2}/*sbd*^{2} carrying two copies of the protease-disabled S737A transgene were collected as white prepupae, aged at 25° until 27.5 hr AP, and then either heat shocked at 37° for 1 hr (hs1) or maintained at 25° (no hs). Another set of *Sb*^{63b} pupae carrying the wild-type transgene was heat shocked at 24, 26, and 28 hr AP (hs2). After heat shock, pupae were returned to 25° until eclosion. Adults were scored for wt, *sbd*, *Sb*, or intermediate (int) phenotype bristles (*n*: number of adults; % wt, sbd, Sb, or int: percentage of each phenotype observed).

produced bristles intermediate between *sbd*^{2} and wild-type length (data not shown). Two copies of the *hs-Sb*$^+$ transgene induced at 27.5 hr AP also rescued the more severe recessive bristle mutation, *sbd*^{201}, with 90% rescue of bristles to wild type and 10% to bristles intermediate between *sbd*^{201} and wild-type length. Because of the high incidence of lethality in the *sbd*^{201} homozygotes, *sbd*^{201}/*Df sbd*^{105} animals were used for these experiments. Bristles of the dominant mutant *Sb*^{63}/+ were not rescued by the wild-type transgene even with multiple heat shocks throughout early bristle development (24–30 hr AP). A single heat shock at 27.5 hr AP rescued bristles of the milder dominant mutant *Sb*^{spike}/+ to wild type in 19% of the treated flies, while another 27% had bristles intermediate between *Sb*^{spike} and wild type. No rescue was evident in 38% of the *Sb*^{spike}/+ heat-shocked flies. These results confirm the identity of the *Sb-sbd* gene and are consistent with genetic predictions that *sbd*^{2} is a hypomorph, that *sbd*^{201}, although recessive, is an antimorph, and that *Sb* dominant mutants are neomorphs (*Sb*^{63b}) or antimorphs (*Sb*^{spike}).

Rescue of leg phenotypes: To rescue mlf legs in *Sb-sbd* mutants, the wild-type *Sb-sbd* transgene was induced by a 1 hr 37° heat shock at the white prepupal stage (0 hr AP), corresponding to the time when the *Sb-sbd* gene is normally expressed in prepupal development. Results from these experiments are summarized in Table 3. Induction of the wild-type transgene increased the occurrence of wild-type legs in both *sbd*^{201} homozygotes and deficiency heterozygotes [*sbd*^{201}/*Df(3R)sbd*^{105}] carrying two copies of the wild-type transgene. A single copy of the wild-type *Sb-sbd* transgene in *sbd*^{201} deficiency heterozygotes [*hs-Sb-sbd*$^+$/+; *sbd*^{201}/*Df(3R)sbd*^{105}] rescued mlf legs more effectively than two copies did, suggesting that leg morphogenesis is sensitive to overexpression of wild-type *Sb-sbd*. In preliminary experiments no rescue of malformed legs in the dominant *Sb* mutants *Sb*^{1}/*Df(3R)sbd*^{105} or *Sb*^{spike}/*Df(3R)sbd*^{105} was produced by induction of the wild-type *Sb-sbd* transgene at 0 hr AP using two copies of the transgene or in *Sb*^{63b}/*Df(3R)sbd*^{105} with either one or two copies (data not shown). This was unexpected, given that the mlf syndrome is recessive, and indicates a functional difference between the defect in the *sbd*^{201} stubblin and the *Sb* mutant stubblins despite similar leg phenotypes in these mutants. It is possible that some endogenous *Sb-sbd* transcription precedes the 0-hr-AP induction of the wild-type transgene, so that mutant stubblin is already present and the heat-shock-induced wild-type stubblin is too late to rescue mlf legs in the *Sb* mutants. Alternatively, or additionally, "collateral damage" of overexpression of *Sb-sbd* could mask rescue of the specific *Sb* leg morphogenesis defect. The improved rescue of *sbd*^{201}/*Df(3R)sbd*^{105} with one compared to two copies of the wild-type transgene supports the argument that there are deleterious effects of overexpression of *Sb-sbd*.

Overexpression of hs-Sb-sbd$^+$ in wild-type flies: To investigate the effects of overexpression of wild-type *Sb-sbd*, the *hs-Sb-sbd*$^+$ transgene was induced at other times throughout prepupal and pupal development in

TABLE 3

Rescue of mlf legs by heat-shock induction of the wild-type *Sb-sbd* transgene

Genotype	Treatment	Leg phenotypes n	% mlf	% wt
hs-Sb$^+$/*hs-Sb*$^+$; *sbd*^{201}/*sbd*^{201}	+hs	63	68	32
	−hs	85	89	11
hs-Sb$^+$/*hs-Sb*$^+$; *sbd*^{201}/*Df(3R)sbd*^{105}	+hs	72	67	33
	−hs	58	93	7
hs-Sb$^+$/+; *sbd*^{201}/*Df(3R)sbd*^{105}	+hs	117	54	46
	−hs	118	91	9
+/+; *sbd*^{201}/*sbd*^{201}	+hs	52	94	6
	−hs	88	96	4
S737A/+; *sbd*^{201}/*Df(3R)sbd*^{105}	+hs	121	100	0
	−hs	122	93	7

White prepupae from *sbd*^{201}/*sbd*^{201} or *sbd*^{201}/*Df (3R) sbd*^{105} stocks carrying zero (+/+), one (*hs-Sb*$^+$/+), or two (*hs-Sb*$^+$/*hs-Sb*$^+$) copies of the wild-type *Sb-sbd* transgene or one copy of the S737A protease-disabled transgene were either heat shocked for 1 hr at 37° immediately after collection at 0 hr AP (+hs) or maintained at 25° (−hs). Adults were scored for the mlf leg phenotype. The number scored (n) and percentage with mlf (% mlf) and wt (% wt) phenotypes are shown.

TABLE 4

Overexpression of wild-type *Sb-sbd* causes defects in leg morphogenesis

Genotype	Treatment	n	% wt
hs-Sb$^+$/*hs-Sb*$^+$; +/+	0 hr AP hs	118	54
	3 hr AP hs	58	50
	30 and 33 hr AP hs	55	0
	No hs	120	100
No transgene	0 hr AP hs	88	96
	3 hr AP hs	56	93
	30 and 33 hr AP hs	70	100
	No hs	70	100

White prepupae from wild-type flies carrying two copies of the wild-type *Sb-sbd* transgene (hs-Sb$^+$) or no transgene were heat shocked immediately (0 hr AP hs) or aged at 25° until 3 hr AP and then heat shocked (3 hr AP). A third group was heat shocked at 30 hr and again at 33 hr AP (30 and 33 hr AP). All heat shocks were at 37° for 1 hr. Adults (n) were scored for leg phenotype. The percentage of individuals with all wild-type legs (no legs malformed) is shown (% wt). See text for a description of differences between malformed leg phenotypes resulting from early and late heat shock.

wild-type animals (Table 4). Induction of *hs-Sb-sbd*$^+$ at 0 hr AP or 3 hr AP produced malformed legs. After a 3-hr-AP heat shock, only 50% of the treated flies developed wild-type legs (the other 50% developed mlf) compared to 96% of the no-transgene control animals. With a 0-hr-AP-only heat shock, 41% of the treated flies had wild-type legs compared to 93% of the no-transgene controls. These observations are similar to those made by Bayer *et al.* (2003). This effect was not seen in prepupal heat shocks after 4 hr AP. Induction of *hs-Sb-sbd*$^+$ during pupal development with a double heat shock at 30 hr AP and 33 hr AP produced a different and unanticipated phenotype (Figure 4). All segments of all legs in these flies are shortened, with severity increasing on a distal-to-proximal axis. First and third legs are more severely affected than second legs. In addition to the leg phenotype, there are defects in cuticle on the dorsal thorax (not shown), including a mild cleft and disorientation of the bristles similar to the phenotypes of mutations that affect thoracic closure (Usui-Ishihara *et al.* 2000; Pena-Rangel *et al.* 2002). The bristle morphology and length are normal. A single heat shock at 27.5 hr AP, which rescued *sbd* bristles, produced a slight shortening of prothoracic femurs, but otherwise wild-type flies. Heat shocks after 42 hr AP, after secretion of the adult cuticle, produced no leg or thoracic phenotype.

Expression of the protease-disabled transgene in wild-type and *Sb-sbd* mutant flies: To determine if an intact protease domain is required for rescue of *Sb-sbd* loss-of-function mutations or overexpression effects, we

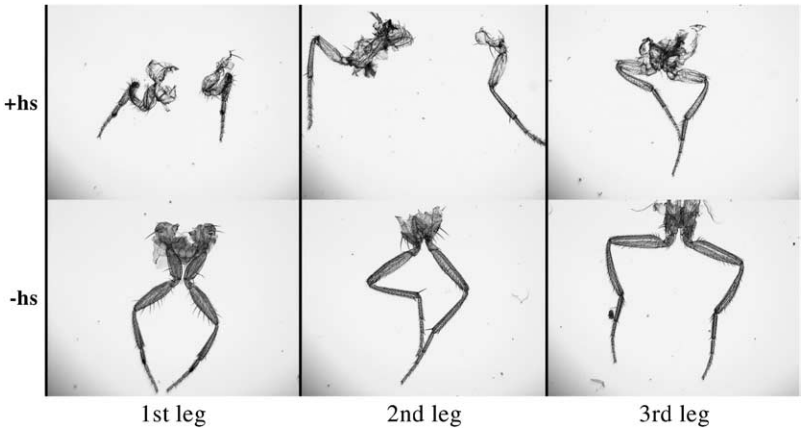

Figure 4.—Leg effects of *Sb-sbd* overexpression in pupae in the first (1st), second (2nd), and third (3rd) legs of adults from pupae carrying two copies of the *hs-Sb-sbd*$^+$ transgene either with (+hs) or without (−hs) a double heat shock at 30 and 33 hr AP. Note short proximal segments decreasing in severity from femur to basitarsis in the legs from heat-shocked pupae. First legs show the most extreme effect.

TABLE 5

Transgenic expression of *Sb-Sbd* truncations or a disabled protease in pupae produces Sb-like bristles

Genotype	Treatment	*n*	% Sb
S737A/S737A; *Df(3R)sbd^{105}*/+	+hs	74	97
	−hs	111	0
Δ*-protease*/Δ*-protease*; *Df(3R)sbd^{105}*/+	+hs	68	44
	−hs	53	4
CD-TM-knot/CD-TM-knot; *Df(3R)sbd^{105}*/+	+hs	75	35
	−hs	89	0
CD-TM/CD-TM; *Df(3R)sbd^{105}*/+	+hs	115	13
	−hs	89	0
+/+; *Df(3R)sbd^{105}*/+	+hs	73	8
	−hs	59	0

Sb-sbd deficiency *trans*-heterozygotes [*Df(3R)sbd^{105}*/+] carrying two copies of the S737A transgene or two copies of one of the truncation transgenes [Δ-protease, CD-TM-knot, CD-TM] or no transgene [+/+; *Df(3R)sbd^{105}*/+] were collected and aged at 25° to 25 hr AP. These pupae were either subjected to four 1-hr heat shocks at 37° (25, 27, 29, and 31 hr AP) with a 1-hr recovery period at 25° between heat shocks (+hs) or maintained at 25° (−hs). Adults (*n*) were scored (% Sb) for bristle phenotype (at least three Sb dorsocentral or scutellar bristles, *i.e.,* blunt-ended bristles <2/3 wt length).

repeated the rescue and overexpression experiments using a transgene with alanine replacing the critical catalytic serine at aa 737 (S737A) to disable the proteolytic function (see Figure 3). This transgene (*hs-Sb-sbd* S737A) was unable to rescue *sbd^{2}* bristles (Table 2) or *sbd^{201}* mlf legs (Table 3). Induction of *hs-Sb-sbd* S737A in wild-type prepupae at 0 hr AP, 3 hr AP, or with a double heat shock at 0 and 3 hr produced no effect on leg morphogenesis (data not shown). Similarly, the leg and cuticle defects seen with the wild-type *Sb-sbd* transgene induced at 30 hr and 33 hr AP were not seen with the protease-disabled transgene, implying a requirement for a functional protease for the overexpression effects as well as for normal leg and bristle morphogenesis.

Generation of Sb bristles by expression the *Sb-sbd* truncation and S737A transgenes: To generate dominant bristle phenotypes similar to those seen with the dominant mutations that make truncated transcripts, we made a series of truncated *Sb-sbd* transgenes (Figure 3). Three transgenic constructs—the truncation deleting the protease domain (Δ-protease) and the truncation deleting the protease and most of the stem, but including the disulfide knot (CD–TM–knot), as well as the S737A mutation—all produced at least some short, thick *Sb*-like bristles when expressed throughout early bristle development. A single heat shock at 27.5 hr did not produce a detectable phenotype. Table 5 shows the results of a series of four heat shocks at 25, 27, 29, and 31 hr AP with two copies of the transgene and a single copy of the endogenous *Sb-sbd* gene. In all cases there was some variation in the bristle phenotype, with the dorsocentral bristles most consistently short. The *hs-Sb-sbd* S737A transgene produced short-bristle phenotypes with highest penetrance and severity; 97% of the heat-shocked pupae produced adults with predominantly short bristles, many shorter than those of *Sb^{1}*. While some of these bristles are both short and thick as in *Sb^{63b}*, some have thick bases with thin extensions, a combination of the *Sb* and *sbd* bristle phenotypes. Figure 5 shows a confocal image of an actin-stained bristle dissected at 37 hr AP from a pupa carrying the S737A transgene induced by heat shock at 25, 27, 29, and 31 hr AP. Also shown is a bristle dissected from a wild-type pupa (no transgene) heat shocked in parallel. Although there is a dramatic difference in bristle length between these two 37-hr-AP bristles, the short bristle does not show the consistent actin bundle mislocalization and increase in the number of bundles seen in a *Sb^{63b}* bristle, *i.e.*, 25–30 bundles not restricted to the cell periphery in *Sb^{63b}* homozyogtes compared to 12–15 solely peripheral bundles in wild-type bristles (Appel *et al.* 1993). The more consistent and severe phenotype may require the constant and abundant presence of the truncated protein in bristles as suggested by the difference in bristle phenotype between *Sb^{1}*, in which the truncated *Sb^{1}* transcript is expressed in amounts comparable to the wild-type transcript, and *Sb^{63b}*, in which the similarly truncated transcript is overexpressed compared to the wild-type transcript. *Sb^{1}* bristles are longer than those of *Sb^{63b}* and while *Sb^{1}* bristles often have extra actin bundles, the number of bundles (11–18) overlaps with that of wild type (Lees and Picken 1945; Overton 1967).

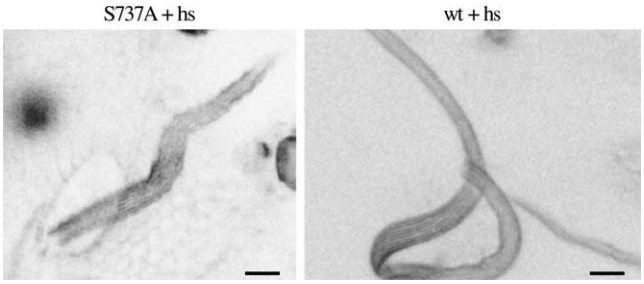

Figure 5.—Sb-like bristle generated by expression of the S737A transgene. Confocal image (negative image) of phalloidin-stained bristles dissected from pupae at 37 hr AP following heat shocks at 25, 27, 29, and 31 hr AP. (Left) An Sb-like bristle from an S737A transgene-carrying pupa [S737A/S737A; *Df(3R)sbd^{105}*/+]. (Right) A normal bristle from a wild-type control pupa (wt) also subjected to the same heat-shock regimen. The tip of the much longer wild-type bristle cannot be seen in this view. The entire S737A bristle is shown. Bars, 5 μm.

The bristle effects of transgenes expressing only the cytoplasmic domain with the transmembrane domain (CD–TM) were indistinguishable from heat-shocked

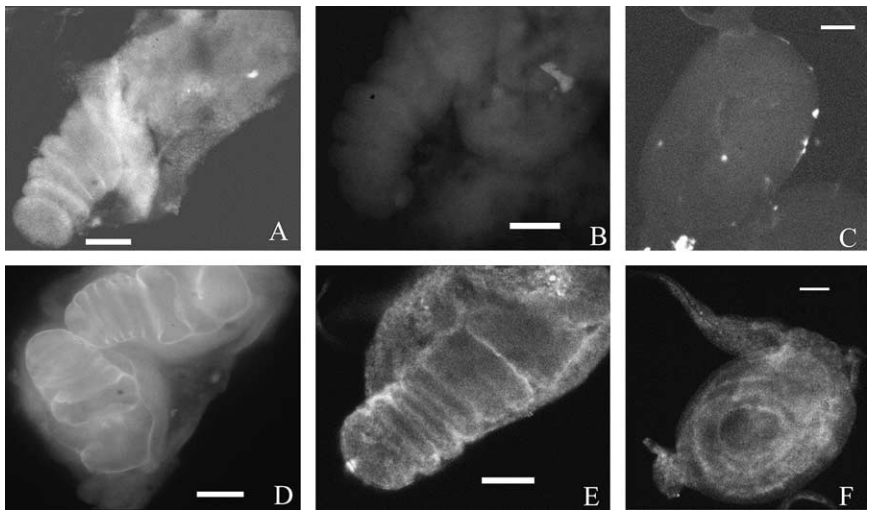

FIGURE 6.—Larval and prepupal leg discs stained with stubblin antistem antiserum. (A and E) Wild-type leg discs dissected at 3.5 hr AP show staining at the apical surface. (E) A confocal image; (A–D and F) conventional epifluorescence. (B) Negative control (no primary antibody). (D) Sb^{63b}/Sb^{63b} leg discs dissected at 3.5 hr AP show a similar pattern but more intense staining, consistent with the overexpression of the Sb^{63b} transcript. Sb^{63b}/Sb^{63b} discs have not elongated as far as their wild-type counterparts. (C and F) Larval discs dissected prior to normal endogenous *Sb-sbd* expression from animals carrying two copies of the wild-type *Sb-sbd* transgene: (C) larvae with no heat shock and (F) larvae heat shocked for 60 min at 37°. Heat-shocked larvae show precocious apical expression, visible as concentric rings in the uneverted disc. Bars, 50 μm.

lines without any transgene (*w; sbd*^{105}/+), even when the copy number of the transgene was increased to 3 (*w/hs-Sb CD-TM;hs-Sb CD-TM/ hs-Sb CD-TM: sbd*^{105}/+). However, because we cannot confirm expression of these shorter constructs with our antibody to the stubblin stem, these results must be considered preliminary. Pupal heat shocks with the wild-type transgene resulted in adults with wild-type bristle length but with severe leg and thorax malformations (Table 4 and data not shown). No leg or thorax effects were seen with any of the truncations or the S737A substitution.

Localization of stubblin in discs: Cell-shape change occurring at the apical surface during prepupal morphogenesis is driven by actin–myosin contractility (CONDIC *et al.* 1991). Previously, we reported that an antibody to the juxtamembrane region of stubblin localized to the apical surface in prepupal discs, consistent with a direct role for stubblin in apical cell-shape change (VON KALM *et al.* 1995). We repeated this localization using a new antiserum made against a nonrepetitive region of the stem (see Figure 3) with similar results (Figure 6, A, B, and E). This antiserum also stains prepupal discs from Sb^{63b} homozygotes, but more intensely, as predictable from the overexpression of the Sb^{63b} transcript (Figure 6D). At 3.5 hr AP, the Sb^{63b} discs already are clearly shorter than their wild-type counterparts, although elongation has started. Leg discs from heat-shocked third instar wild-type larvae carrying two copies of the wild-type *Sb-sbd* transgene show precocious apical localization, visible as concentric rings in the unevaginated disc (Figure 6F). Non-heat-shocked controls show no stubblin expression as expected for larval discs prior to the rise in ecdysone titer (Figure 6C).

Localization of stubblin in developing bristles: Because *Sb-sbd* mutants affect the actin bundle scaffolding in growing bristles, it was of interest to determine the localization of stubblin during bristle development when actin bundles are forming. We used the stubblin stem antiserum for immunolocalization studies in bristles from 32 hr AP, when bristle buds first appear, through 38 hr AP, about midway through bristle extrusion. Actin staining of early bristles shows the beginning of actin bundles as punctate staining on the surface of the bristle bud with discrete bundles extending to the base of the shaft (TILNEY *et al.* 1996; WULFKUHLE *et al.* 1998; Figure 7B). In contrast, stubblin staining at 34–35 hr AP shows cytoplasmic staining of the cell body of the bristle shaft cell with diffuse staining of the budding shaft and tip (Figure 7, A and C). By 37 hr AP, stubblin staining is more concentrated at the tips, indicating that stubblin is transferred to the tip (Figure 7D). From our micrographs, we cannot rule out that the early staining seen at the bristle base is in the socket cell, but because extruding bristle shafts clearly show stubblin staining, we argue by parsimony that expression is restricted to the shaft cell. Sb^{63b} bristles at 37 hr AP are shorter than their wild-type counterparts but stain in a similar pattern except the staining is more intense, with the appearance of heavily staining cap-like extensions on the tips (Figure 8). These localization patterns of stubblin in growing bristles, distinct from those of actin, particularly in sprouting bristles when actin bundles are first detectable, indicate that the actin bundle defects seen in *Sb-sbd* mutants do not result from a direct interaction of stubblin with actin bundles. The cap of stubblin that appears at the ends of Sb^{63b} bristles suggests the possibility that an accumulation of defective stubblin at the bristle tips may block bristle extension, consistent with the *Sb* bristle phenotype of abruptly terminated bristles.

DISCUSSION

The ecdysone-induced *Sb-sbd* gene is required for normal morphogenesis of imaginal discs and formation of bristle shafts, both processes involving cytoskeletal

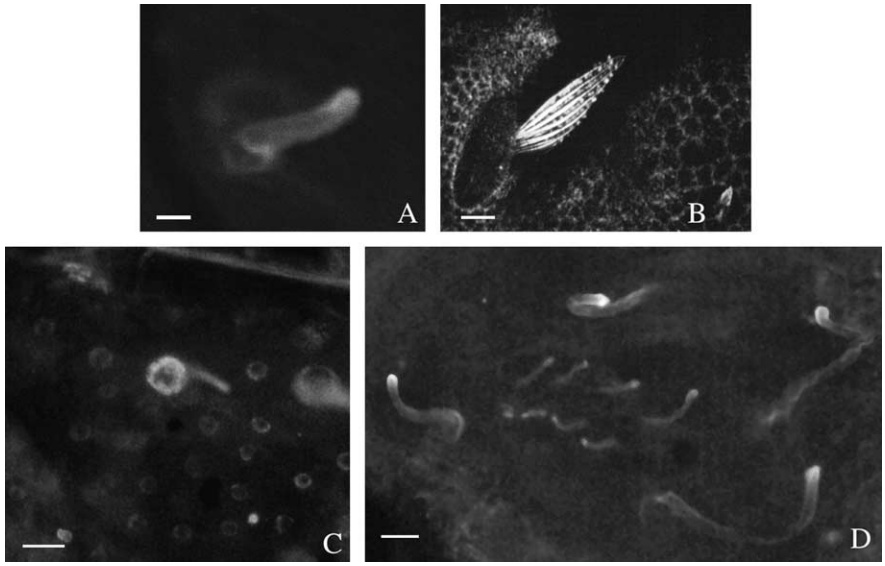

Figure 7.—Stubblin localization in developing bristles. Bristles from 34- to 37-hr-AP pupae stained with stubblin stem antiserum (A, C, and D) or phalloidin (B). Confocal images of individual early bristles (~34 hr AP) show distinct staining patterns for stubblin (A) compared to actin (B). (C) A field of bristles from a 36-hr-AP pupa (conventional epifluorescence) shows bristle base, shaft, and tip stubblin staining of macrochaetes. Smaller microchaetes, which develop slightly after macrochaetes, still show predominate bristle base staining, visible as rings. Confocal image of a field of bristles from a 37-hr-AP pupa shows an increased concentration of stubblin at the growing bristle tips (D). Image in B from Dianne Fristrom. Bars: A and B, 5 μm; C and D, 20 μm.

changes and extracellular proteolytic activity. The morphogenesis of the leg imaginal disc to form a tubular leg depends on myosin-driven contraction leading to apical cell-shape change. In contrast, formation of bristles is driven by polymerization of membrane-associated, parallel actin filaments. We discuss here the possible roles of *Sb-sbd* in imaginal disc morphogenesis and bristle extrusion and speculate that the stubblin protease modifies apical ECM and contributes, directly or indirectly, to activation of a Rho-signaling pathway.

The role of *Sb-sbd* in leg disc morphogenesis: Morphogenesis of leg imaginal discs requires both contraction of the apical actin–myosin contractile ring and proteolysis. In rapid response to the ecdysone spike that triggers metamorphosis, the shapes of cells in the distal femur, tibia, and basitarsis change from elongated to isometric (Condic *et al.* 1991). If these changes are blocked, the resulting legs in the adult fly are malformed with short and thick proximal segments. Genetical and cell biological observations lead to the view that leg morphogenesis depends on myosin-driven contractility. Both actin and nonmuscle myosin II localize to the apical belt in leg discs (von Kalm *et al.* 1995). Cytochalasins, which disrupt actin filaments, reversibly inhibit leg disc elongation (Fristrom and Fristrom 1975). Mutations in the *zip* gene, which encodes the nonmuscle myosin II heavy chain, cause the mlf phenotype as do those of the myosin regulatory light chain gene, *spaghetti squash* (*sqh*) (Edwards and Kiehart 1996).

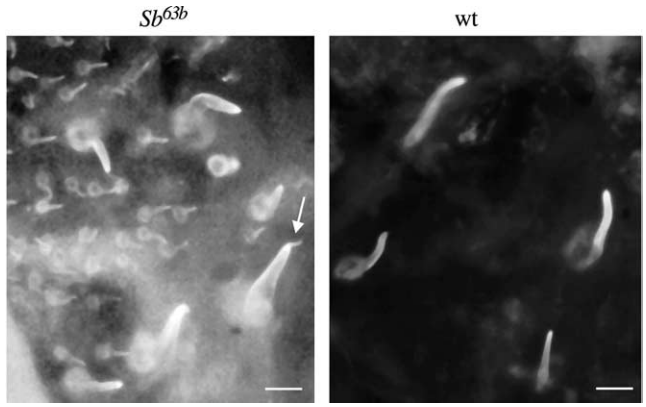

Figure 8.—Wild-type and Sb^{63b}/+ bristles from 36-hr-AP pupae stained with stubblin stem antiserum. Both show stubblin protein localized to bristle cell base, shaft, and tip, but Sb^{63b} staining is more intense, with heavily staining tip extensions (arrow) not seen in the wild-type bristles. Bars, 20 μm.

Contractility alone is insufficient for leg morphogenesis. The leg disc epithelium is covered by a basal ECM similar to those of vertebrates, containing collagen IV, laminin, and sulfated proteoglycans (Fessler and Fessler 1989; Fristrom and Fristrom 1993). The disc apical surface secretes a chitinous cuticle (exoskeleton) during metamorphosis. Epidermal morphogenesis, including leg elongation during prepupal morphogenesis and bristle formation during pupal morphogenesis, must occur when the epidermis is unconstrained by the exoskeleton. Prepupal leg elongation occurs between pupariation and the formation of the pupal chitinous exoskeleton (Fristrom and Fristrom 1993). Apolysis of the pupal cuticle at ~18 hr AP allows further leg morphogenesis and formation of bristles and hairs before the adult exoskeleton is deposited between 36 to 70 hr AP. After apolysis, the apical surface of the disc secretes a poorly characterized, fibrous, nonchitinous ECM (Brower *et al.* 1987; Fristrom and Fristrom 1993). A role for proteolysis in disc morphogenesis is well documented. In addition to *Sb-sbd*, other proteases known to be regulated by ecdysone and potentially involved in disc morphogenesis include an unidentified extracellular protease secreted by cultured discs in response to ecdysone (Pino-Heiss and Schubiger

1989) and a collagenase that cleaves type IV collagen (Birr *et al.* 1990; Fessler *et al.* 1993). Disc morphogenesis is restricted by protease inhibitors (Pino-Heiss and Schubiger 1989). It is accelerated *in vitro* by exogenous trypsin or chymotrypsin (Poodry and Schneiderman 1971; Fekete *et al.* 1975). Addition of 0.1% trypsin to the *in vitro* medium decreases the time of leg elongation of dissected discs from 2–3 hr to 10 min, but only in discs that have been exposed to ecdysone (Fekete *et al.* 1975). Protease treatment does not passively lead to leg elongation; trypsin acceleration of leg elongation is inhibited under conditions that reduce ATP levels and does not overcome cytochalasin B inhibition of disc elongation (Fekete *et al.* 1975). Thus, contractility and proteolysis must be coordinated for normal morphogenesis to occur. Stubblin, the product of ecdysone-dependent *Sb-sbd* and a TTSP that localizes to the apical surface of leg discs, is a candidate for one of the coordinators.

A role for *Sb-sbd* in leg morphogenesis was first described by Dobzhansky (1929) and rediscovered because of the genetic interaction between *Sb-sbd* and the metamorphic transcriptional regulator, *br*, to produce mlf legs (Beaton *et al.* 1988). The legs of some *Sb-sbd* homozyogtes, *Sb-sbd trans*-hetereozygotes, or *br; Sb-sbd/+* double mutants are mlf. Leg morphogenesis in these mutants can be rescued *in vitro* by exposure to exogenous trypsin in prepupal discs (Appel *et al.* 1993). Our current studies show that induction of the wild-type *Sb-sbd* transgene early in prepupal development (0 hr AP) partially rescued severe sbd^{201}/sbd^{201} mlf legs, but not alleles with dominant bristle phenotypes (Sb^{1}, Sb^{63b}, Sb^{spike}). Rescue depends on the presence of a functional protease catalytic domain; the catalytically disabled S737A transgene did not rescue mlf legs. One copy of the wild-type transgene rescued more animals than two copies (50% rescue *vs.* 30%), demonstrating that overexpression of wild-type stubblin has deleterious effects on leg development. Expression of the wild-type transgene in wild-type animals during prepupal development resulted in adults with mlf legs, confirming the sensitivity of leg morphogenesis to overexpression of stubblin. Overexpression of protease *in vivo* may result in excess detachment of epidermis from the apical ECM, compromising the structural integrity of the elongated leg and causing malformations even if cell-shape changes are completed. Relevant here is our observation that some stubblin overexpression phenotypes resulting from induction of the wild-type *Sb-sbd* transgene in wild-type prepupae (0 and 3 hr AP) were not identical to "classic" mlf. While "classic" mlf legs associated with limited cell-shape changes have short, kinked femurs, primarily on the metathoracic legs (see Beaton *et al.* 1988, Figure 1), prepupal overexpression of stubblin also produced some longer, fragile mesothoracic and metathoracic legs that arguably could result from excessive leg elongation like that seen *in vitro* with protease exposure (Fekete *et al.* 1975).

Myosin II contractility depends on the phosphorylation state of myosin regulatory light chain (MLC) (Tan *et al.* 1992; Amano *et al.* 1996). Numerous studies point to the Rho subfamily of small GTPases as upstream regulators of the actin cytoskeletal rearrangements and control of MLC phosphorylation (Tapon and Hall 1997; Van Aelst and D'Souza-Schorey 1997; Ridley 2001). Recent genetic interaction studies have identified members of a potential Rho-signaling pathway that may lead to the contraction of the actin–myosin apical belt and the cell-shape changes that drive prepupal leg disc morphogenesis. Rho-signaling pathway components implicated in Drosophila disc morphogenesis include *RhoGEF2* and *RhoA* (Halsell *et al.* 2000; Ward *et al.* 2003) and Drosophila *Rho kinase* (*drok*) (Winter *et al.* 2001). Mutations in these genes interact with *zip* mutations to produce mlf legs (Gotwals and Fristrom 1991; Halsell *et al.* 2000; Bayer *et al.* 2003). Activators upstream of *RhoA* in leg morphogenesis have not been identified. The possibility that *Sb-sbd* is involved in this or a parallel pathway is suggested by the mlf leg phenotype of *Sb-sbd* mutations in combination with *zip* mutations (Gotwals and Fristrom 1991) or with mutations of *RhoA*, *RhoGEF2*, or *drok* genes (Bayer *et al.* 2003; Ward *et al.* 2003).

Any consideration of the mechanism of action of the *Sb-sbd* gene in imaginal disc morphogenesis must take into account the nature of the morphogenetic defects associated with *Sb-sbd* mutations. The proteolytic domain of stubblin is essential for normal morphogenesis. Stubblin in sbd^{201}/sbd^{201}, which has an arguably impaired catalytic domain, and stubblin molecules lacking the proteolytic domain (in Sb^{63b}, Sb^{70}, and Sb^{1}) are associated with abnormalities in disc morphogenesis. Models for roles of the proteolytic domain are all speculative because the stubblin substrate is unknown. The possibility that stubblin may directly or indirectly modify the apical ECM has been suggested often (Beaton *et al.* 1988; Appel *et al.* 1993; von Kalm *et al.* 1995; Hooper *et al.* 2001; Bayer *et al.* 2003) and is supported by the acceleration of leg elongation caused by exogenous trypsin, the *in vitro* rescue of partially elongated Sb^{63b}/Sb^{63b} leg discs by trypsin, and the apical localization of stubblin in leg discs. However, stubblin may have a dual role both in modifying the ECM to permit cell-shape change and in stimulating the contractility of the apical contractile belt, for example, by activating a Rho-signaling pathway. Because morphogenesis begins in *Sb* mutants that are missing the protease domain, stubblin cannot be acting alone to initiate contractility, but may be required to amplify a signal to complete morphogenesis.

As a transmembrane protease, stubblin is a candidate for a membrane-associated activator of RhoA, transducing an outside-to-inside signal either directly, through its own intracellular domain, or indirectly, through cleavage of another cell-surface protein that activates Rho signaling (see also Bayer *et al.* 2003). The first possibility

is unlikely because the stubblin cytoplasmic domain lacks identified protein interaction motifs, and our preliminary studies suggest that overexpression of the SbCD or SbCD-TM transgenes has no effect on leg morphogenesis. Regarding the second possibility, serine proteases that, like stubblin, use the Ser-His-Asp catalytic triad can be classified according to highly conserved evolutionary markers on the basis of codon usage at Ser195 and Ser214 and the presence of Pro *vs.* Tyr at residue 225 (chymotrypsin numbering) (Krem and Di Cera 2001). According to this classification system, stubblin belongs to the oldest lineage and therefore is more likely, on the basis of analysis of other proteolytic cascades, to be the terminal or penultimate protease in an activation cascade and less likely to be an initiator (Krem and Di Cera 2001). To speculate briefly, a protease-activated receptor (PAR) could be a stubblin substrate. PARs belong to a family of G-protein-coupled receptors that are activated by site-specific proteolysis (Dery *et al.* 1998). Several other TTSP proteases have been demonstrated to activate protease-activated receptor-2 (PAR-2) (Lin *et al.* 1999; Takeuchi *et al.* 2000; Friedrich *et al.* 2002; Iwakiri *et al.* 2004; Wilson *et al.* 2005). Proteolytic modification of ECM attachments not only may be permissive, but also may actively contribute to Rho-mediated signaling. Future studies must focus on the identification of stubblin substrates.

The role of *Sb-sbd* in bristle morphogenesis: Bristle formation involves actin polymerization but not myosin II contractility. The first bristle nubs appear at ~32 hr AP, during a period of high ecdysone titer, and extend to their full length by 48 hr AP (Lees and Waddington 1942; Fristrom and Fristrom 1993). Bristles grow from the tip (Lees and Picken 1945). The bristle elongates by the assembly of membrane-associated, cross-linked actin filament bundles formed in short modules, new bundles being joined end to end with the preceding more basal bundle (Tilney *et al.* 1996; Guild *et al.* 2003). From observations of bristle growth in cultured thoraces in the presence of compounds that effect actin polymerization or microtubule dynamics, Tilney *et al.* (2000, 2003) concluded that actin polymerization drives bristle elongation. Unlike leg disc morphogenesis, bristle development is not affected by mutations in *zip* and these mutations do not interact with *Sb-sbd* mutations to affect bristle elongation (Bayer *et al.* 2003). In the bristles of recessive *sbd* animals, the actin bundles are normal at first, but stop prematurely and asynchronously, so that some bundles continue to extend, while others stop. The resulting bristles are shorter than wild-type bristles and have ragged ends instead of smooth, tapered ends. This defect was rescued by the wild-type *Sb-sbd* transgene in both the mild allele sbd^{2} and the more severe allele sbd^{201}. The molecular defect in sbd^{201}, a histidine-to-arginine substitution at aa 571 in the catalytic domain, is likely to compromise but not abolish protease activity (see RESULTS). In contrast to the results with mlf leg rescue, complete rescue of sbd^{201} or sbd^{2} bristles required two copies of the *hs-Sb-sbd*$^{+}$ transgene, a single copy resulting in partial rescue (intermediate length bristles). Only the transgene with an intact protease domain rescued bristles. Unlike legs, bristles are not sensitive to overexpression of wild-type stubblin.

Identification of molecular defects in *Sb* dominant mutations, Sb^{63b} and Sb^{70}, showed that truncated, protease-absent stubblin causes the severe dominant bristle phenotypes. The bristles in these mutants and those in Sb^{1}, another dominant mutant associated with a transposable element eliminating the protease domain, were not rescued by the wild-type transgene, and so these three mutations are likely to be neomorphs, acting in some novel way not characteristic of the wild-type protein. The bristle phenotype of the milder allele Sb^{spike}, a frameshift mutation that adds sequence to the C terminus of the protease domain and likely disrupts normal stubblin function, was ameliorated by the wild-type transgene, although not rescued completely to wild-type length. Induction of transgenes truncated to remove the protease domain and then progressively larger portions of the noncatalytic region showed dominant effects from expression of truncated protein as short as the CD–TM–knot construct. The most penetrant and severe phenotypes were produced by the S737A construct, which changes only the catalytic serine. Consistent with the difference in the dominant and recessive character of *Sb* and *sbd* mutations in bristle and legs, none of the truncation transgenes had any effects on leg morphogenesis. Taken together, these observations indicate a role for the stubblin noncatalytic domains that is specific to bristle elongation. The localization pattern of stubblin in bristles brings up the possibility that the stem or knot may be involved in localization of the protease to the bristle tip, although this is not directly testable with our antiserum to the C-terminal region of the stem. Stubblin appears first in the budding bristle cell body (and perhaps in the socket cell) and then along the shaft to the bristle tip where it concentrates. Immunolocalization with the stubblin stem antiserum in Sb^{63b}/+ developing bristles showed excessive accumulation of protein at the bristle tips compared to the normal protein in wild-type bristles. If the noncatalytic domains direct stubblin localization, expression of a truncated Sb^{63b} or Sb^{1} protein may block wild-type stubblin proteolytic function. The observation that overexpression of the wild-type *Sb-sbd* transgene fails to rescue the bristle phenotype of these mutants suggests that either the transgenic stubblin is inefficiently transported or the interference is irreversible. The requirement for two copies of the wild-type transgene for bristle rescue of even the mildest *sbd* mutation indicates that bristle elongation depends on a sufficient concentration of protease. This extremely long (400-μm) cytoplasmic projection may require concentration

of a protease at the bristle tip to facilitate bristle extrusion through the apical ECM. If so, it would suggest that stubblin protease either directly cleaves an apical ECM component or activates another protease that does so. A role for stubblin in relieving ECM constraint is consistent with the accumulation of stubblin at the bristle tips and the increasing growth rate as bristles get longer (Tilney *et al.* 2000).

The extra and mislocated actin bundles in Sb^{63b} bristles suggest a possible role for neomorphic stubblin in regulation of actin bundle initiation (Appel *et al.* 1993). The actin filament membrane connector in bristles is unknown. On the basis of the localization pattern of stubblin in bristles, which is distinctly different from that of actin, it is unlikely that stubblin interacts directly with actin. Stubblin could, however, activate another more spatially restricted signal similarly to the mechanism proposed for the TTSP enteropeptidase (see Kong *et al.* 1997). Recently, Tilney *et al.* (2004) reported evidence for the influence of external forces (pupal cuticle and placement of the dendrite) and internal forces (actin bundling, actin assembly, and actin bundle positioning) on bristle shape and length. We propose that ECM constraint is an additional external force in bristle morphogenesis. Lees and Picken (1945), Overton (1967), and Tilney *et al.* (2003) all found that the total bristle volume is the same in wild-type and *Sb* mutants; the increased bundle number and thickness in the mutants corresponds to the decrease in length. The extra bundles are most numerous in severe dominant mutants that produce a truncated protein entirely lacking the stubblin protease, *e.g.*, Sb^{63b} (Appel *et al.* 1993). One interpretation of these observations is that bundle formation continues in *Sb* bristles, but the bristle cannot extend without the action of the protease on the restricting apical ECM so the modules accumulate within the stunted bristle cell. In addition, neomorphic stubblin in severe *Sb* mutants indirectly causes, through the acquisition of a new function mediated by the stem domains, increased assembly of actin bundles. In *sbd* mutants that retain any protease function, *e.g.*, sbd^{2} or sbd^{201} homozygotes, actin bundles can extend in "holes" where stubblin is active, resulting in the observed nonuniform termination of the actin bundles (Appel *et al.* 1993). Hypothetically, in *sbd* nulls, bristle growth would be severely restrained but extra bundles would not form.

By what mechanisms could wild-type stubblin have roles in regulating the internal force of actin assembly as well as in modifying the ECM to permit extension? Like leg morphogenesis, bristle extension requires the coordinated action of cytoskeletal change and ECM proteolysis. However, other than the requirement for stubblin, the molecular mechanisms in leg and bristle development differ. Studies on the formation of yeast cables have identified formin homology (FH) proteins as nucleators specific to the assembly of parallel, unbranched actin filaments, like those that drive bristle extension (Evangelista *et al.* 2002; Pruyne *et al.* 2002; Sagot *et al.* 2002). Several FH proteins have been found to interact with the Rho GTPases, suggesting that FH proteins may act as Rho effectors that communicate RhoGTPase signals to the cytoskeleton (Kohno *et al.* 1996; Imamura *et al.* 1997; Watanabe *et al.* 1997). To extend the model proposed above for the function of stubblin in legs, one can speculate that in bristle development regulation of actin filament polymerization requires an FH protein and a Rho GTPase that is activated by a PAR receptor. Expressed at the tips of growing bristles, stubblin could activate a more spatially restricted PAR or PAR activator and proteases that release the apical ECM attachments around the bristle tip, again linking cytoskeletal changes to ECM modification. Clarification of the roles of stubblin will require the identification of stubblin substrates and other interacting proteins, while keeping in mind that stubblin substrates may differ during disc morphogenesis and bristle elongation. Recent genetic screens (Bayer *et al.* 2003; Ward *et al.* 2003), which have identified several new *Sb-sbd* alleles and genetic interactors, could facilitate this search.

We thank Cindy Bayer and Laurie von Kalm for helpful discussions, for their collaboration in construction of the transgenic stocks, and for their critical comments on the manuscript. We are grateful to Dianne Fristrom for sharing her expertise in disc dissection, immunohistochemistry, and microscopy, and for the image in Figure 7B. We are indebted to David King for his advice on peptide antigens and for synthesis of the peptide used to generate the stubblin stem antiserum. We thank Charles Craik for his insightful comments on the potential impact of the sbd^{201} mutation on stubblin protease function. We also appreciate the efforts of two anonymous reviewers whose comments improved the manuscript. This work was supported in part by grants from the National Science Foundation (IBN-9630783) and the National Institutes of Health (GM50264).

LITERATURE CITED

Abu-Shumays, R., 1995 The characterization of two 20 hydroxyecdysone regulated genes in *Drosophila* imaginal discs. Ph.D. Thesis, University of California, Berkeley, CA.

Adams, M. D., S. E. Celniker, R. A. Holt, C. A. Evans, J. D. Gocayne *et al.*, 2000 The genome sequence of Drosophila melanogaster. Science **287:** 2185–2195.

Amano, M., M. Ito, K. Kimura, Y. Fukata, K. Chihara *et al.*, 1996 Phosphorylation and activation of myosin by Rho-associated kinase (Rho-kinase). J. Biol. Chem. **271:** 20246–20249.

Appel, L. F., 1992 The cloning and characterization of *Stubble-stubbloid*, a morphogenetic locus in *Drosophila*. Ph.D. Thesis, University of California, Berkeley, CA.

Appel, L. F., M. Prout, R. Abu-Shumays, A. Hammonds, J. C. Garbe *et al.*, 1993 The Drosophila Stubble-stubbloid gene encodes an apparent transmembrane serine protease required for epithelial morphogenesis. Proc. Natl. Acad. Sci. USA **90:** 4937–4941.

Bayer, C. A., S. R. Halsell, J. W. Fristrom, D. P. Kiehart and L. von Kalm, 2003 Genetic interactions between the RhoA and Stubble-stubbloid loci suggest a role for a type II transmembrane serine protease in intracellular signaling during Drosophila imaginal disc morphogenesis. Genetics **165:** 1417–1432.

Beaton, A. H., I. Kiss, D. Fristrom and J. W. Fristrom, 1988 Interaction of the Stubble-stubbloid locus and the Broad-complex of *Drosophila melanogaster*. Genetics **120:** 453–464.

Bingham, P. M., and C. H. Chapman, 1986 Evidence that white-blood is a novel type of temperature-sensitive mutation resulting

from temperature-dependent effects of a transposon insertion on formation of white transcripts. EMBO J. **5:** 3343–3351.

Birr, C. A., D. Fristrom, D. S. King and J. W. Fristrom, 1990 Ecdysone-dependent proteolysis of an apical surface glycoprotein may play a role in imaginal disc morphogenesis in Drosophila. Development **110:** 239–248.

Bode, W., P. Schwager and R. Huber, 1978 The transition of bovine trypsinogen to a trypsin-like state upon strong ligand binding. The refined crystal structures of the bovine trypsinogen-pancreatic trypsin inhibitor complex and of its ternary complex with Ile-Val at 1.9 A resolution. J. Mol. Biol. **118:** 99–112.

Brower, D. L., M. Piovant, R. Salatino, J. Brailey and M. J. Hendrix, 1987 Identification of a specialized extracellular matrix component in Drosophila imaginal discs. Dev. Biol. **119:** 373–381.

Chen, G. C., P. Gajowniczek and J. Settleman, 2004 Rho-LIM kinase signaling regulates ecdysone-induced gene expression and morphogenesis during Drosophila metamorphosis. Curr. Biol. **14:** 309–313.

Clark, H. F., D. Brentrup, K. Schneitz, A. Bieber, C. Goodman *et al.*, 1995 Dachsous encodes a member of the cadherin superfamily that controls imaginal disc morphogenesis in Drosophila. Genes Dev. **9:** 1530–1542.

Condic, M. L., D. Fristrom and J. W. Fristrom, 1991 Apical cell shape changes during Drosophila imaginal leg disc elongation: a novel morphogenetic mechanism. Development **111:** 23–33.

Dery, O., C. U. Corvera, M. Steinhoff and N. W. Bunnett, 1998 Proteinase-activated receptors: novel mechanisms of signaling by serine proteases. Am. J. Physiol. **274:** C1429–C1452.

Dobzhansky, T., 1929 The manifold effects of the genes Stubble and stubbloid in *Drosophila melanogaster*. Z. Indukt. Abstamm. Vererbungsl. **54:** 427–457.

Edwards, K. A., and D. P. Kiehart, 1996 Drosophila nonmuscle myosin II has multiple essential roles in imaginal disc and egg chamber morphogenesis. Development **122:** 1499–1511.

Evangelista, M., D. Pruyne, D. C. Amberg, C. Boone and A. Bretscher, 2002 Formins direct Arp2/3-independent actin filament assembly to polarize cell growth in yeast. Nat. Cell Biol. **4:** 260–269.

Fekete, E., D. Fristrom, I. Kiss and J. W. Fristrom, 1975 The mechanism of evagination of imaginal discs of Drosophila melanogaster II. Studies on trypsin-accelerated evagination. Roux's Arch. Dev. Biol. **178:** 123–138.

Fessler, J. H., and L. I. Fessler, 1989 Drosophila extracellular matrix. Annu. Rev. Cell Biol. **5:** 309–339.

Fessler, L. I., M. L. Condic, R. E. Nelson, J. H. Fessler and J. W. Fristrom, 1993 Site-specific cleavage of basement membrane collagen IV during Drosophila metamorphosis. Development **117:** 1061–1069.

Friedrich, R., P. Fuentes-Prior, E. Ong, G. Coombs, M. Hunter *et al.*, 2002 Catalytic domain structures of MT-SP1/matriptase, a matrix-degrading transmembrane serine proteinase. J. Biol. Chem. **277:** 2160–2168.

Fristrom, D., 1988 The cellular basis of epithelial morphogenesis. A review. Tissue Cell **20:** 645–690.

Fristrom, D., and J. W. Fristrom, 1975 The mechanism of evagination of imaginal discs of Drosophila melanogaster. 1. General considerations. Dev. Biol. **43:** 1–23.

Fristrom, D., and J. Fristrom, 1993 The metamorphic development of the adult epidermis, pp. 843–897 in *The Development of Drosophila melanogaster*, edited by M. Bate and A. Martinez-Arias. Cold Spring Harbor Laboratory Press, Cold Spring Harbor, NY.

Frohman, M. A., 1993 Rapid amplification of complementary DNA ends for generation of full-length complementary DNAs: thermal RACE. Methods Enzymol. **218:** 340–356.

Furie, B., and B. C. Furie, 1988 The molecular basis of blood coagulation. Cell **53:** 505–518.

Gates, J., and C. S. Thummel, 2000 An enhancer trap screen for ecdysone-inducible genes required for Drosophila adult leg morphogenesis. Genetics **156:** 1765–1776.

Gay, N. J., and F. J. Keith, 1992 Regulation of translation and proteolysis during the development of embryonic dorso-ventral polarity in Drosophila. Homology of easter proteinase with Limulus proclotting enzyme and translational activation of Toll receptor synthesis. Biochim. Biophys. Acta **1132:** 290–296.

Gotwals, P. J., and J. W. Fristrom, 1991 Three neighboring genes interact with the Broad-Complex and the Stubble-stubbloid locus to affect imaginal disc morphogenesis in Drosophila. Genetics **127:** 747–759.

Guild, G. M., P. S. Connelly, K. A. Vranich, M. K. Shaw and L. G. Tilney, 2002 Actin filament turnover removes bundles from Drosophila bristle cells. J. Cell Sci. **115:** 641–653.

Guild, G. M., P. S. Connelly, L. Ruggiero, K. A. Vranich and L. G. Tilney, 2003 Long continuous actin bundles in Drosophila bristles are constructed by overlapping short filaments. J. Cell Biol. **162:** 1069–1077.

Halsell, S. R., B. I. Chu and D. P. Kiehart, 2000 Genetic analysis demonstrates a direct link between rho signaling and nonmuscle myosin function during Drosophila morphogenesis. Genetics **155:** 1253–1265.

Hammonds, A. S., 2002 Mutational analysis of Drososphila *Stubble-stubbloid* gene function in ecdysone-regulated morphogenesis. Ph.D. Thesis, University of California, Berkeley, CA.

Hartenstein, V., and J. W. Posakony, 1989 Development of adult sensilla on the wing and notum of Drosophila melanogaster. Development **107:** 389–405.

Hooper, J. D., J. A. Clements, J. P. Quigley and T. M. Antalis, 2001 Type II transmembrane serine proteases. Insights into an emerging class of cell surface proteolytic enzymes. J. Biol. Chem. **276:** 857–860.

Imamura, H., K. Tanaka, T. Hihara, M. Umikawa, T. Kamei *et al.*, 1997 Bni1p and Bnr1p: downstream targets of the Rho family small G-proteins which interact with profilin and regulate actin cytoskeleton in Saccharomyces cerevisiae. EMBO J. **16:** 2745–2755.

Iwakiri, K., M. Ghazizadeh, E. Jin, M. Fujiwara, T. Takemura *et al.*, 2004 Human airway trypsin-like protease induces PAR-2-mediated IL-8 release in psoriasis vulgaris. J. Invest. Dermatol. **122:** 937–944.

Jiang, H., and M. R. Kanost, 2000 The clip-domain family of serine proteinases in arthropods. Insect Biochem. Mol. Biol. **30:** 95–105.

Kohno, H., K. Tanaka, A. Mino, M. Umikawa, H. Imamura *et al.*, 1996 Bni1p implicated in cytoskeletal control is a putative target of Rho1p small GTP binding protein in Saccharomyces cerevisiae. EMBO J. **15:** 6060–6068.

Kong, W., K. McConalogue, L. M. Khitin, M. D. Hollenberg, D. G. Payan *et al.*, 1997 Luminal trypsin may regulate enterocytes through proteinase-activated receptor 2. Proc. Natl. Acad. Sci. USA **94:** 8884–8889.

Krem, M. M., and E. Di Cera, 2001 Molecular markers of serine protease evolution. EMBO J. **20:** 3036–3045.

Lees, A. D., and L. E. R. Picken, 1945 Shape in relation to the fine structure in the bristles of *Drosophila melanogaster*. Proc. R. Soc. Lond. Ser. B **132:** 396–423.

Lees, A. D., and C. H. Waddington, 1942 The development of bristles in normal and some mutant types of *Drosophila melanogaster*. Proc. R. Soc. Lond. Ser. B **131:** 87–110.

Lewis, E. B., 1948 New mutants. Dros. Inf. Ser. **22:** 72–73.

Lin, C. Y., J. Anders, M. Johnson, Q. A. Sang and R. B. Dickson, 1999 Molecular cloning of cDNA for matriptase, a matrix-degrading serine protease with trypsin-like activity. J. Biol. Chem. **274:** 18231–18236.

Lindsley, D. L., and E. H. Grell, 1968 *Genetic Variations of Drosophila melanogaster*. Pub. 627, Carnegie Institute, Washington, DC.

Madison, E. L., A. Kobe, M. J. Gething, J. F. Sambrook and E. J. Goldsmith, 1993 Converting tissue plasminogen activator to a zymogen: a regulatory triad of Asp-His-Ser. Science **262:** 419–421.

Moore, W. G., 1935 New mutants. Dros. Inf. Ser. **3:** 27.

Muta, T., R. Hashimoto, T. Miyata, H. Nishimura, Y. Toh *et al.*, 1990 Proclotting enzyme from horseshoe crab hemocytes. cDNA cloning, disulfide locations, and subcellular localization. J. Biol. Chem. **265:** 22426–22433.

Muta, T., T. Nakamura, R. Hashimoto, T. Morita and S. Iwanaga, 1993 Limulus proclotting enzyme. Methods Enzymol. **223:** 352–358.

Nelson, C. R., and P. Szauter, 1992 Cytogenetic analysis of chromosome region 89A of Drosophila melanogaster: isolation of deficiencies and mapping of Po, Aldox-1 and transposon insertions. Mol. Gen. Genet. **235:** 11–21.

Netzel-Arnett, S., J. D. Hooper, R. Szabo, E. L. Madison, J. P. Quigley *et al.*, 2003 Membrane anchored serine proteases: a rapidly expanding group of cell surface proteolytic enzymes with potential roles in cancer. Cancer Metastasis Rev. **22:** 237–258.

Overton, J., 1967 The fine structure of developing bristles in wild type and mutant Drosophila melanogaster. J. Morphol. **122:** 367–379.

Pena-Rangel, M. T., I. Rodriguez and J. R. Riesgo-Escovar, 2002 A misexpression study examining dorsal thorax formation in *Drosophila melanogaster*. Genetics **160:** 1035–1050.

Pino-Heiss, S., and G. Schubiger, 1989 Extracellular protease production by Drosophila imaginal discs. Dev. Biol. **132:** 282–291.

Poodry, C. A., and H. A. Schneiderman, 1971 Intercellular adhesivity and pupal morphogenesis in *Drosophila melanogaster*. Roux's Arch. Dev. Biol. **168:** 1–9.

Pruyne, D., M. Evangelista, C. Yang, E. Bi, S. Zigmond *et al.*, 2002 Role of formins in actin assembly: nucleation and barbed-end association. Science **297:** 612–615.

Rawlings, N. D., D. P. Tolle and A. J. Barrett, 2004 MEROPS: the peptidase database. Nucleic Acids Res. **32:** D160–D164.

Ridley, A. J., 2001 Rho family proteins: coordinating cell responses. Trends Cell Biol. **11:** 471–477.

Rubin, G. M., and A. C. Spradling, 1982 Genetic transformation of Drosophila with transposable element vectors. Science **218:** 348–353.

Sagot, I., S. K. Klee and D. Pellman, 2002 Yeast formins regulate cell polarity by controlling the assembly of actin cables. Nat. Cell Biol. **4:** 42–50.

Smith, C. L., and R. DeLotto, 1992 A common domain within the proenzyme regions of the Drosophila snake and easter proteins and Tachypleus proclotting enzyme defines a new subfamily of serine proteases. Protein Sci. **1:** 1225–1226.

Smith, C., H. Giordano and R. DeLotto, 1994 Mutational analysis of the Drosophila snake protease: an essential role for domains within the proenzyme polypeptide chain. Genetics **136:** 1355–1365.

Takeuchi, T., J. L. Harris, W. Huang, K. W. Yan, S. R. Coughlin *et al.*, 2000 Cellular localization of membrane-type serine protease 1 and identification of protease-activated receptor-2 and single-chain urokinase-type plasminogen activator as substrates. J. Biol. Chem. **275:** 26333–26342.

Tan, J. L., S. Ravid and J. A. Spudich, 1992 Control of nonmuscle myosins by phosphorylation. Annu. Rev. Biochem. **61:** 721–759.

Tapon, N., and A. Hall, 1997 Rho, Rac and Cdc42 GTPases regulate the organization of the actin cytoskeleton. Curr. Opin. Cell Biol. **9:** 86–92.

Thummel, C. S., 1997 Dueling orphans: interacting nuclear receptors coordinate Drosophila metamorphosis. BioEssays **19:** 669–672.

Thummel, C. S., 2002 Ecdysone-regulated puff genes 2000. Insect Biochem. Mol. Biol. **32:** 113–120.

Thummel, C. S., and V. Pirrotta, 1992 New pCaSpeR P element vectors. Dros. Inf. Ser. **71:** 150.

Tilney, L. G., M. S. Tilney and G. M. Guild, 1995 F actin bundles in Drosophila bristles. I. Two filament cross-links are involved in bundling. J. Cell Biol. **130:** 629–638.

Tilney, L. G., P. Connelly, S. Smith and G. M. Guild, 1996 F-actin bundles in Drosophila bristles are assembled from modules composed of short filaments. J. Cell Biol. **135:** 1291–1308.

Tilney, L. G., P. S. Connelly, K. A. Vranich, M. K. Shaw and G. M. Guild, 1998 Why are two different cross-linkers necessary for actin bundle formation in vivo and what does each cross-link contribute? J. Cell Biol. **143:** 121–133.

Tilney, L. G., P. S. Connelly, K. A. Vranich, M. K. Shaw and G. M. Guild, 2000 Actin filaments and microtubules play different roles during bristle elongation in Drosophila. J. Cell Sci. **113** (Pt. 7): 1255–1265.

Tilney, L. G., P. S. Connelly, L. Ruggiero, K. A. Vranich and G. M. Guild, 2003 Actin filament turnover regulated by cross-linking accounts for the size, shape, location, and number of actin bundles in Drosophila bristles. Mol. Biol. Cell **14:** 3953–3966.

Tilney, L. G., P. S. Connelly, L. Ruggiero, K. A. Vranich, G. M. Guild *et al.*, 2004 The role actin filaments play in providing the characteristic curved form of Drosophila bristles. Mol. Biol. Cell **15:** 5481–5491.

Usui-Ishihara, A., P. Simpson and K. Usui, 2000 Larval multidendrite neurons survive metamorphosis and participate in the formation of imaginal sensory axonal pathways in the notum of Drosophila. Dev. Biol. **225:** 357–369.

Van Aelst, L., and C. D'Souza-Schorey, 1997 Rho GTPases and signaling networks. Genes Dev. **11:** 2295–2322.

von Kalm, L., D. Fristrom and J. Fristrom, 1995 The making of a fly leg: a model for epithelial morphogenesis. BioEssays **17:** 693–702.

Ward, R. E., J. Evans and C. S. Thummel, 2003 Genetic modifier screens in Drosophila demonstrate a role for Rho1 signaling in ecdysone-triggered imaginal disc morphogenesis. Genetics **165:** 1397–1415.

Watanabe, N., P. Madaule, T. Reid, T. Ishizaki, G. Watanabe *et al.*, 1997 p140mDia, a mammalian homolog of Drosophila diaphanous, is a target protein for Rho small GTPase and is a ligand for profilin. EMBO J. **16:** 3044–3056.

Wilson, S., B. Greer, J. Hooper, A. Zijlstra, B. Walker *et al.*, 2005 The membrane-anchored serine protease, TMPRSS2, activates PAR-2 in prostate cancer cells. Biochem. J. **388:** 967–972.

Winter, C. G., B. Wang, A. Ballew, A. Royou, R. Karess *et al.*, 2001 Drosophila Rho-associated kinase (Drok) links Frizzled-mediated planar cell polarity signaling to the actin cytoskeleton. Cell **105:** 81–91.

Wulfkuhle, J. D., N. S. Petersen and J. J. Otto, 1998 Changes in the F-actin cytoskeleton during neurosensory bristle development in Drosophila: the role of singed and forked proteins. Cell Motil. Cytoskeleton **40:** 119–132.

Communicating editor: K. V. Anderson